

NASA TECHNICAL NOTE



NASA TN D-7019

C.1

NASA TN D-7019

LOAN COPY: RETURN TO
AFWL (DOGL)
KIRTLAND AFB, NM



GASEOUS-HELIUM REQUIREMENTS FOR
THE DISCHARGE OF LIQUID HYDROGEN
FROM A 3.96-METER- (13-FT-) DIAMETER
SPHERICAL TANK

*by Robert J. Stochl, Joseph E. Maloy,
Phillip A. Masters, and Richard L. DeWitt*

*Lewis Research Center
Cleveland, Ohio 44135*



0133716

| | | | |
|--|--|---|---------------------------------|
| 1. Report No. NASA TN D-7019 | 2. Government Accession No. | 3. Recipient's Catalog No. | |
| 4. Title and Subtitle GASEOUS-HELIUM REQUIREMENTS FOR THE DISCHARGE OF LIQUID HYDROGEN FROM A 3.96-METER-(13-FT-) DIAMETER SPHERICAL TANK | | 5. Report Date December 1970 | 6. Performing Organization Code |
| | | 8. Performing Organization Report No. E-5797 | 10. Work Unit No. 180-31 |
| 7. Author(s) Robert J. Stochl, Joseph E. Maloy, Phillip A. Masters, and Richard L. DeWitt | | 11. Contract or Grant No. | |
| | | 13. Type of Report and Period Covered Technical Note | |
| 9. Performing Organization Name and Address Lewis Research Center National Aeronautics and Space Administration Cleveland, Ohio 44135 | | 14. Sponsoring Agency Code | |
| | | 12. Sponsoring Agency Name and Address National Aeronautics and Space Administration Washington, D.C. 20546 | |
| 15. Supplementary Notes | | | |
| 16. Abstract An experimental investigation was conducted to determine the effects of various physical parameters on the pressurant gas (gaseous helium) requirements during the pressurization and expulsion of liquid hydrogen from a 3.96-meter- (13-ft-) diameter spherical tank. The experimental results were also compared with results predicted by a previously developed analytical program. The experimental results show that the inlet gas temperature has a strong influence on the actual pressurant gas requirements. There is an average decrease in pressurant gas requirements of 1.0 percent for a 10 K (18° R) increase in inlet gas temperature. The analytical program was able to predict the actual pressurant requirements to within a maximum of 4.6 percent for all cases. | | | |
| 17. Key Words (Suggested by Author(s)) Pressurization Pressurized expulsion Gaseous helium pressurant Cryogenic propellant tanks | | 18. Distribution Statement Unclassified - unlimited | |
| 19. Security Classif. (of this report) Unclassified | 20. Security Classif. (of this page) Unclassified | 21. No. of Pages 61 | 22. Price* \$3.00 |

GASEOUS-HELIUM REQUIREMENTS FOR THE DISCHARGE OF
LIQUID HYDROGEN FROM A 3.96-METER- (13-FT-)
DIAMETER SPHERICAL TANK

by Robert J. Stochl, Joseph E. Maloy, Phillip A. Masters,
and Richard L. DeWitt

Lewis Research Center

SUMMARY

An experimental investigation was conducted to determine the effects of various physical parameters on the pressurant gas (gaseous helium, GHe) requirements during the pressurization and expulsion of liquid hydrogen from a 3.96-meter - (13-ft-) diameter spherical tank. The experimental results were compared with results predicted by a previously developed analytical program. Tests were conducted for a range of liquid outflow rates, pressurizing rates, and initial ullage volumes at a nominal operating pressure of 34.47×10^4 newtons per square meter (50 psia) using nominal inlet gas temperatures of 168 and 300 K (302.4° and 540° R). Data were obtained using a hemisphere injector.

The experimental results show that the inlet gas temperature has a strong influence on the actual pressurant gas requirements. There is an average decrease in pressurant gas requirements of 1.0 percent for a 10 K (18° R) increase in inlet gas temperature. The analytical program was able to predict the actual pressurant requirements to within a maximum of 4.6 percent for all cases.

INTRODUCTION

During the past several years, a great deal of effort has been devoted to the problems associated with the pressurized discharge of a cryogenic liquid from a tank. The main objectives of these efforts have been toward the optimization of a propellant tank pressurization system. One phase of this optimization is a precise determination of pressurant requirements for any given set of operating parameters (i. e., tank pressure,

inlet gas temperature, liquid outflow rate, tank size, etc.). This knowledge would allow the design of a system that carried only the weight (pressurant gas and associated tankage) necessary to accomplish the mission.

Several investigators have developed analyses (e. g. , refs. 1 and 2) that attempt to predict, according to a selected set of simplifying assumptions, the quantity of pressurant gas required during the pressurized discharge of liquid hydrogen (LH₂). Some of these simplifying assumptions may, for certain conditions (i. e. , for various injector geometries, tank shapes, and sizes) limit the capability of the analysis to accurately predict pressurant requirements. Because of these limitations, the validity of the analytical results have to be largely based on correlations with experimental results.

An experimental investigation was started at Lewis Research Center to determine the effects of various physical parameters on the pressurant gas requirements during the pressurization and expulsion of liquid hydrogen from propellant tanks. The experimental results were also used to extend the capability of the analysis of reference 1 to predict the pressurant requirements for tanks of general geometry under various operating conditions. Some results of this program are reported in references 3 to 6.

This report presents a continuation of the investigation to determine the effect of inlet gas temperature and liquid outflow rate on the helium pressurant requirements in a large spherical tank. Similar tests were reported in reference 6 using a smaller (1.52-m; 5-ft) diameter tank. This report uses the same modifications to the original analysis (ref. 1) that were used in reference 6. For convenience, these modifications are presented in appendixes A to C.

The primary objective of the test work described herein was to obtain experimental values of the pressurant gas requirements during the pressurization and expulsion period in a 3.96-meter- (13-ft-) diameter spherical tank for the various operating parameters and to compare these values with (1) values obtained using hydrogen as the pressurant gas (ref. 5), (2) values obtained in a 1.52-meter- (5-ft-) diameter tank using helium as the pressurant (ref. 6), and (3) values predicted by the analytical program. A secondary objective was to obtain experimental information on tank wall heating, liquid heating, residual ullage energy, and mass transfer in order to gain an insight into the reasons for any variations in pressurant gas requirements.

The tests were conducted using a spherical aluminum tank mounted in a vacuum chamber. The main test variables were (1) nominal inlet gas temperatures of 168 K (302.4° R) and 300 K (540° R), and (2) liquid outflow rates between 1.73 and 4.32 kilograms per second (3.81 and 9.52 lb/sec). When a specific impulse of 444 seconds is used, the low and high flow rates correspond to thrust levels of 25 361 and 112 752 newtons (10 150 and 45 153 lb), respectively. All tests were conducted at a tank pressure of 34.47×10^4 newtons per square meter (50 psia) using a hemisphere injector. Data were also obtained for pressurization of the tank from 1 atmosphere to the operating

level at various rates from 2.48×10^3 to 8.96×10^3 newtons per square meter per second (0.36 to 1.30 psi/sec) for initial tank ullages of 5, 28, 55, and 75 percent of total tank volume.

SYMBOLS

| | |
|------------|--|
| A | area, m^2 (ft^2) |
| b | $1 - \frac{Z_1}{Z} - 2 \frac{\Delta r}{r_i}$ |
| C | orifice coefficient |
| C_H | effective perimeter of interior hardware, m (ft) |
| C_p | specific heat at constant pressure, $J/(kg)(K)$ ($Btu/(lb)(^{\circ}R)$) |
| C_v | specific heat at constant volume, $J/(kg)(K)$ ($Btu/(lb)(^{\circ}R)$) |
| C_w | specific heat of tank wall, $J/(kg)(K)$ ($Btu/(lb)(^{\circ}R)$) |
| c | $\alpha - \alpha\omega - T_w - \frac{1}{l_w \rho_w} \Delta t \frac{\dot{q}}{C_w}$, K ($^{\circ}R$) |
| D | orifice diameter, m (ft) |
| d | $\frac{Z_2 \Delta x}{Z \Delta t} \frac{P' - P}{P'} - \frac{Z_1 \Delta x}{Z \Delta t}$, m/sec (ft/sec) |
| Gr | Grashof number, $\frac{L^3 \rho^2 g \beta \Delta T}{\mu^2}$ |
| g | gravity acceleration, m/sec^2 (ft/sec^2) |
| H | enthalpy, J (Btu) |
| h | specific enthalpy, J/kg (Btu/lb) |
| h_c | convective heat-transfer coefficient, $J/(m^2)(K)(sec)$ ($Btu/(ft^2)(^{\circ}R)(sec)$) |
| k | thermal conductivity, $J/(m)(K)(sec)$ ($Btu/(ft)(^{\circ}R)(sec)$) |
| L | flow length, m (ft) |
| l | thickness, m (ft) |
| M | mass, kg (lb) |
| ΔM | differential mass, kg (lb) |

| | |
|----------------|--|
| \dot{M} | mass flow rate, kg/sec (lb/sec) |
| \bar{M} | molecular weight, kg/(kg)(mole) (lb/(lb)(mole)) |
| M_I | ideal pressurant requirement, kg (lb) |
| N | number of volume segments |
| \bar{N} | number of data points used in defining average deviation |
| Nu | Nusselt number, $\frac{h_c L}{k}$ |
| N_1 to N_Z | particular volume segments |
| n or i | summing index |
| P | pressure, N/m^2 (lb/in. ²) |
| ΔP | differential pressure, N/m^2 (lb/in. ²) |
| ΔP^* | orifice ΔP |
| Pr | Prandtl number, $\frac{\mu C_p}{k}$ |
| Q | heat transfer, J (Btu) |
| \dot{Q} | heat-transfer rate, J/sec (Btu/sec) |
| \dot{Q}' | specific heat-transfer rate, J/(kg)(sec) (Btu/(lb)(sec)) |
| \dot{q} | heat-transfer rate per unit area, J/(m ²)(sec) (Btu/(ft ²)(sec)) |
| R | gas constant, J/(K)(mole) ((ft-lb)/(°R)(mole)) |
| Re | Reynolds number, $\frac{L\bar{V}\rho}{\mu}$ |
| r | radius, m (ft) |
| Δr | increment of radius, m (ft) |
| ΔS | increment of arc length, m (ft) |
| T | temperature, K (°R) |
| ΔT | differential temperature, K (°R) |
| T_δ | temperature at edge of thermal boundary layer, K (°R) |
| t | time, sec |
| Δt | time increment, sec |
| U | internal energy, J (Btu) |

- ΔU differential energy, J (Btu)
 u specific internal energy, J/kg (Btu/lb)
 V volume, m^3 (ft^3)
 ΔV volume increment, m^3 (ft^3)
 \bar{V} velocity, m/sec (ft/sec)
 v specific volume, m^3/kg (ft^3/lb)
 W work, J (Btu)
 X percent of gas by volume
 X_n number of net points in ullage
 x coordinate in direction of tank axis, m (ft)
 Δx space increment, m (ft)
 Y expansion factor
 y thickness within boundary layer, m (ft)
 Z compressibility factor
 z elevation or vertical distance along tank wall, m (ft)

$$\alpha = \frac{1 + \frac{h_c \Delta t}{\rho_w l_w C_w}}{\left(\frac{2h_c R Z \Delta t}{r M P C_p} \right) \left[1 + \left(\frac{\Delta r}{\Delta x} \right)^2 \right]^{1/2}}, \text{ K } (^{\circ}\text{R})$$

- β coefficient of thermal expansion, $1/K$ ($1/^{\circ}\text{R}$)
 γ specific heat ratio
 δ finite increment, or total boundary layer thickness, m (ft)
 λ latent heat of vaporization, J/kg (Btu/lb)
 μ viscosity, $kg/(m)(hr)$ ($lb/(ft)(hr)$)
 ρ density, kg/m^3 (lb/ft^3)
 $\omega = \left(\frac{R}{M} Z_1 \frac{\Delta P}{\Delta t} + \frac{R Z C_H \dot{q}_H}{M \pi r^2} \right) \frac{\Delta t}{C_p P}$

Subscripts:

- A** analytical results

ad adiabatic
 E experimental results
 f final state or condition
 G gas added to tank
 H internal hardware
 He helium
 H₂ hydrogen
 i initial state or condition
 i → f from initial to final state or condition
 L liquid
 n summing index
 o condition prior to ramp
 S liquid surface
 sat saturation
 T total quantity
 t transfer
 t₁, t₂ times 1 and 2
 U ullage
 w wall

Superscripts:

' time index or step forward in time
 * indicates that evaluation may be performed at beginning or end of time interval

Constants for Beattie-Bridgeman equation:

A (N)(m⁴)/kg², (ft⁴/lb)
 a m³/kg, (ft³/lb)
 B m³/kg, (ft³/lb)
 b m³/kg, (ft³/lb)
 C (m³)(K³)/kg, ((ft³)(°R³)/lb)

$$\bar{M} = X_{H_2} \bar{M}_{H_2} + X_{He} \bar{M}_{He}$$

$$\epsilon = (X_{H_2} C_{H_2} + X_{He} C_{He}) / \nu T^3$$

APPARATUS AND INSTRUMENTATION

Facility

All tests were conducted inside a 7.61-meter- (25-ft-) diameter spherical vacuum chamber (fig. 1) to reduce the external heat leak into the propellant tank to a minimum value. The vacuum capability of this chamber was approximately 8×10^{-7} millimeter of mercury. A general schematic of the test tank and associated equipment is shown in figure 2. A heat exchanger and blend valve subsystem capable of delivering gaseous

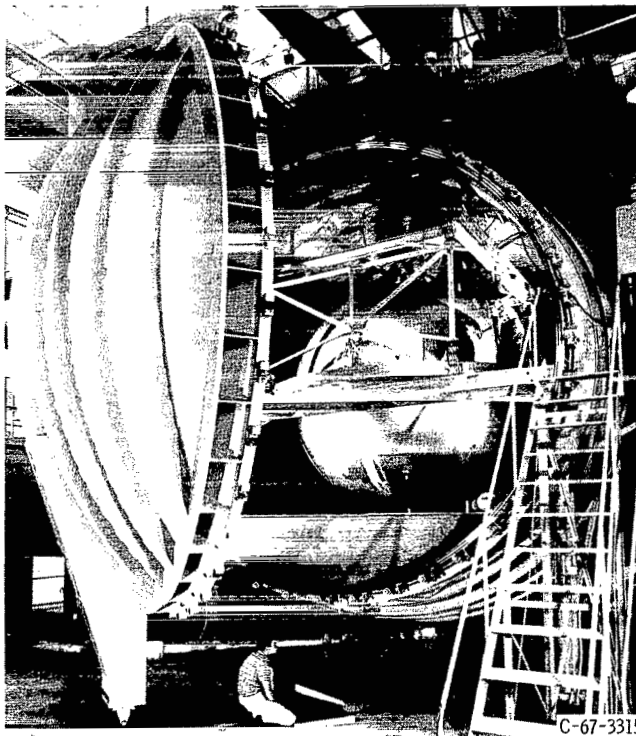


Figure 1. - 3.96-Meter (13-ft) diameter tank installed in 7.61-meter (25-ft) diameter spherical vacuum chamber.

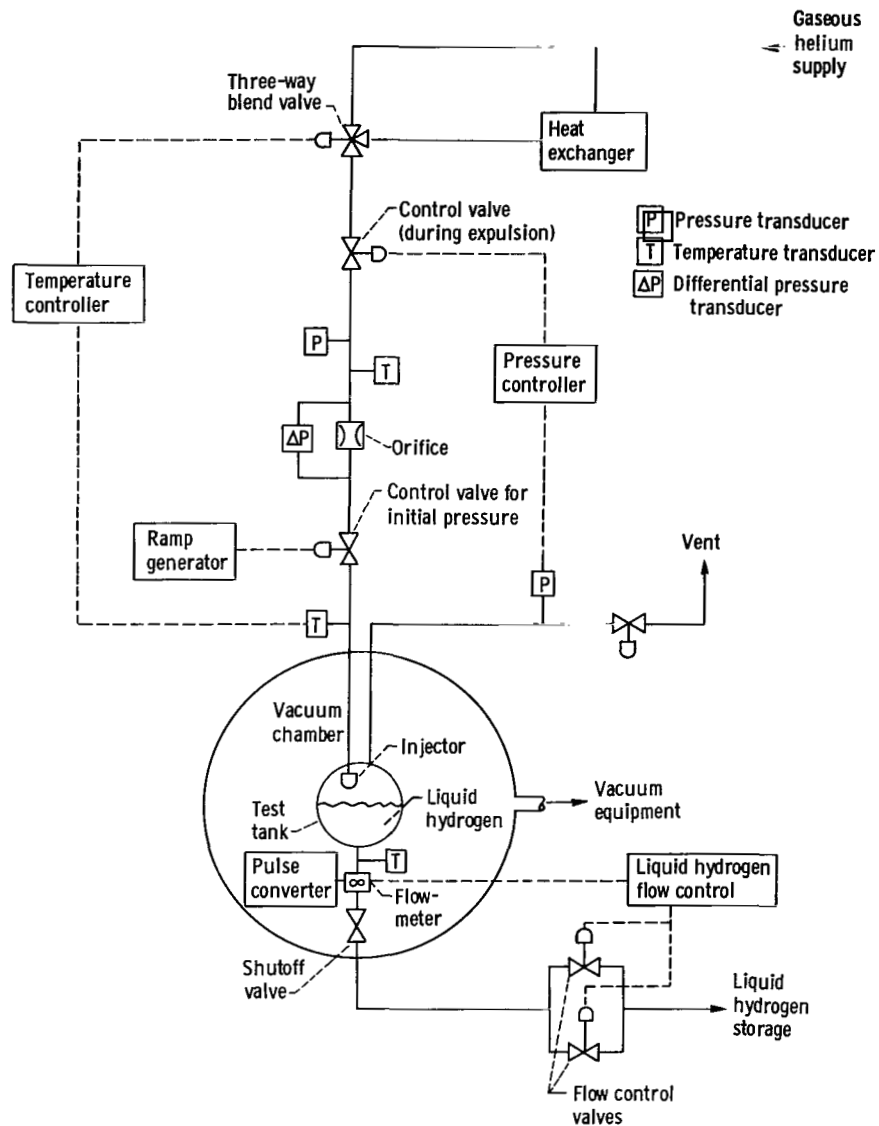


Figure 2. - General facility schematic.

helium at any desired temperature between 167 and 405 K (300^o and 730^o R) at a maximum flow rate of 0.454 kilogram per second (1.00 lb/sec) was used to control pressurant gas inlet temperature. A ramp generator and control valve were used for controlling the initial rate of pressurization of the propellant tank. A closed-loop pressure control circuit was used to maintain constant tank pressure during the expulsion period. The liquid outflow rate was controlled by remotely operated variable flow valves. The liquid hydrogen outflow from the tank was returned to the storage dewar.

Liquid outflow rates were measured using a turbine-type flowmeter located in the transfer line. The flowmeter was calibrated (within an estimated uncertainty of $\pm 1/2$

percent) with liquid hydrogen over the expected range of flow rates. The calibration was performed at Lewis Research Center. Pressurant gas inlet flow rates were determined by the use of an orifice located in the pressurant supply line. Tank, line, and differential pressures were measured with bonded strain-gage transducers (estimated uncertainty of $\pm 1/4$ percent).

All measurements except the gas concentrations were recorded on a high-speed digital data system. The measurements were recorded at a rate of 3.125×10^3 channels per second. Each measurement channel was sampled every 0.064 second.

Test Tank

The experimental work was conducted in a 3.96-meter- (13-ft-) diameter spherical tank. The tank (fig. 3) was constructed of twelve 2219-T87 aluminum alloy gore segments and had an internal volume of 32.0 cubic meters (1130 ft³). Each segment was chem-milled to three thicknesses: The weld land thickness was 1.91 centimeters (0.75 in.), the mid-land was 1.27 centimeters (0.50 in.) thick, and the membrane thickness was 0.89 centimeter (0.35 in.). The tank weight was 1800 kilograms (3969 lb). The proof pressure of the tank was 179×10^4 newtons per square meter (260 psia) with a safety factor of 2. A 0.457-meter- (18-in. -) diameter flanged assembly was used as the lid of the tank. The lid, which housed the inlet and vent pipes and the electrical connections for all internal tank instrumentation, was constructed of 347 stainless steel and weighed 92.08 kilograms (203 lb).

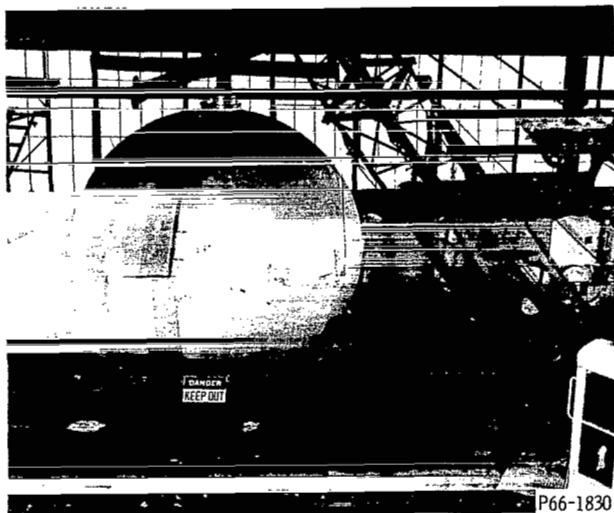


Figure 3. - 3.96-Meter (13-ft) diameter test tank.

Pressurant Gas Injector Geometry

A hemisphere injector (fig. 4) was used for all tests reported herein. The hemisphere injector was selected because it injects the pressurant uniformly in all directions into the ullage volume (minimized ullage gas mixing). The uniform diffusion of pressurant is a basic assumption of the analysis used in this report. The open exit area for the injector was 928 square centimeters (143.9 in.²).

Internal Tank Instrumentation

Temperatures. - Ullage gas temperatures together with gas concentration measurements were used to determine the mass and energy content of the tank ullage. The temperatures must be obtained with sensors capable of accurate measurement of rapid changes in temperature. Internal tank instrumentation is illustrated in figure 5. Location of the vertical and horizontal ullage gas temperature rakes are indicated. The thermopile was the basic temperature measurement technique used in this investigation. The use of thermopiles to measure ullage gas temperature was first developed in reference 7 and the technique was used with good results in references 3 to 6. The main advantage of using thermopiles is their fast response time (between 0.2 and 1.0 sec) in going from saturated liquid to vapor (through a ΔT of approximately 6.1 K (11° R)). This time response is approximately an order of magnitude faster than carbon or platinum resistance sensors which have been used in this type of investigation.

The instrumentation rake (fig. 6(a)) used in this investigation and in reference 5 was an improved version of the rake used in reference 4. The sensors on this rake are more exposed to the surrounding than the sensors of reference 4. Triangular truss sections were used as the main support structure. The trusses were constructed of 0.476-centimeter- (0.187-in.) diameter stainless steel tubing (fig. 6(a)) to minimize the heat capacity of the rake. Interlocking laminated thermoplastic modules were used as the frame for the thermopile sensors.

A typical three-element thermopile unit wiring schematic is illustrated in figure 6(b). The thermopile units were constructed of 0.202-millimeter- (0.008-in.-) chromel-constantan wire. Vertical ullage gas temperature profiles were obtained by stacking the individual thermopile units as shown in figure 6(a). The spacing between the reference and measuring levels was 6.60 centimeters (2.60 in.) for the top 48 thermopiles of the vertical rake. The 8 units at the bottom of the rake had a 3.30-centimeter- (1.30-in.-) spacing in order to obtain a more accurate temperature profile of the ullage gas near the liquid surface at the end of an expulsion.

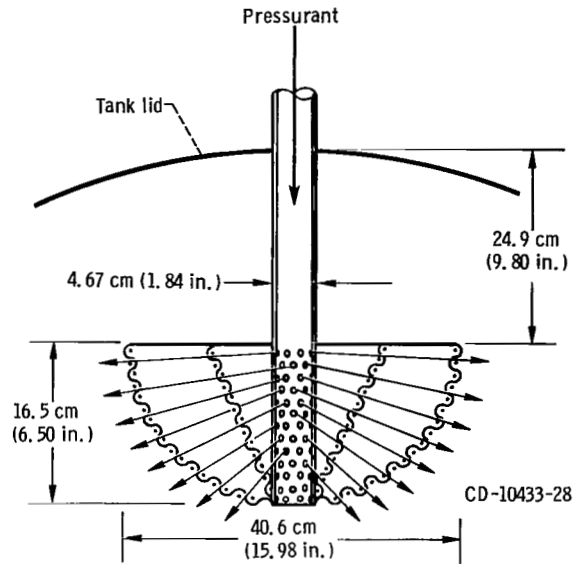


Figure 4. - Hemisphere injector. Open area of outer screen, 928 square centimeters (143.9 in.²)

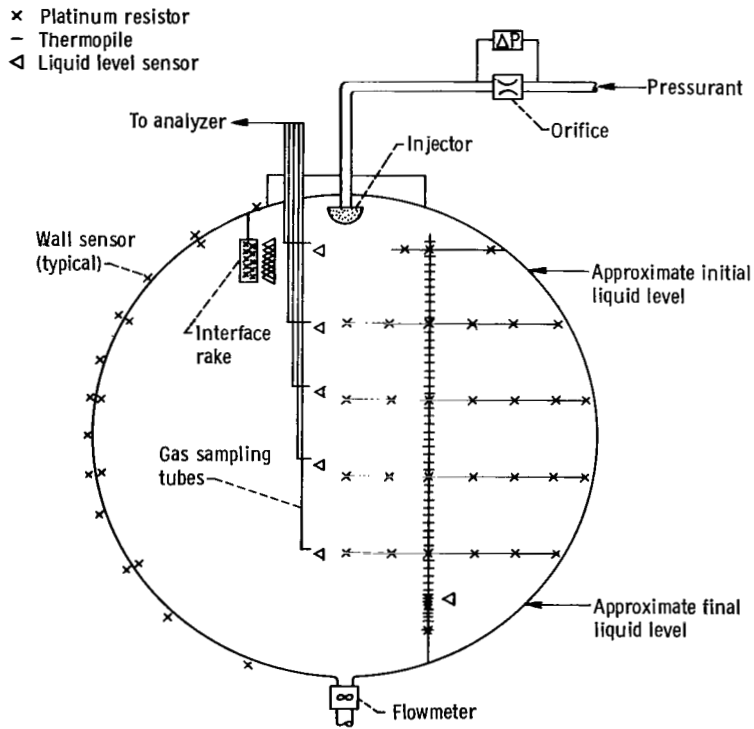


Figure 5. - Test tank instrumentation.

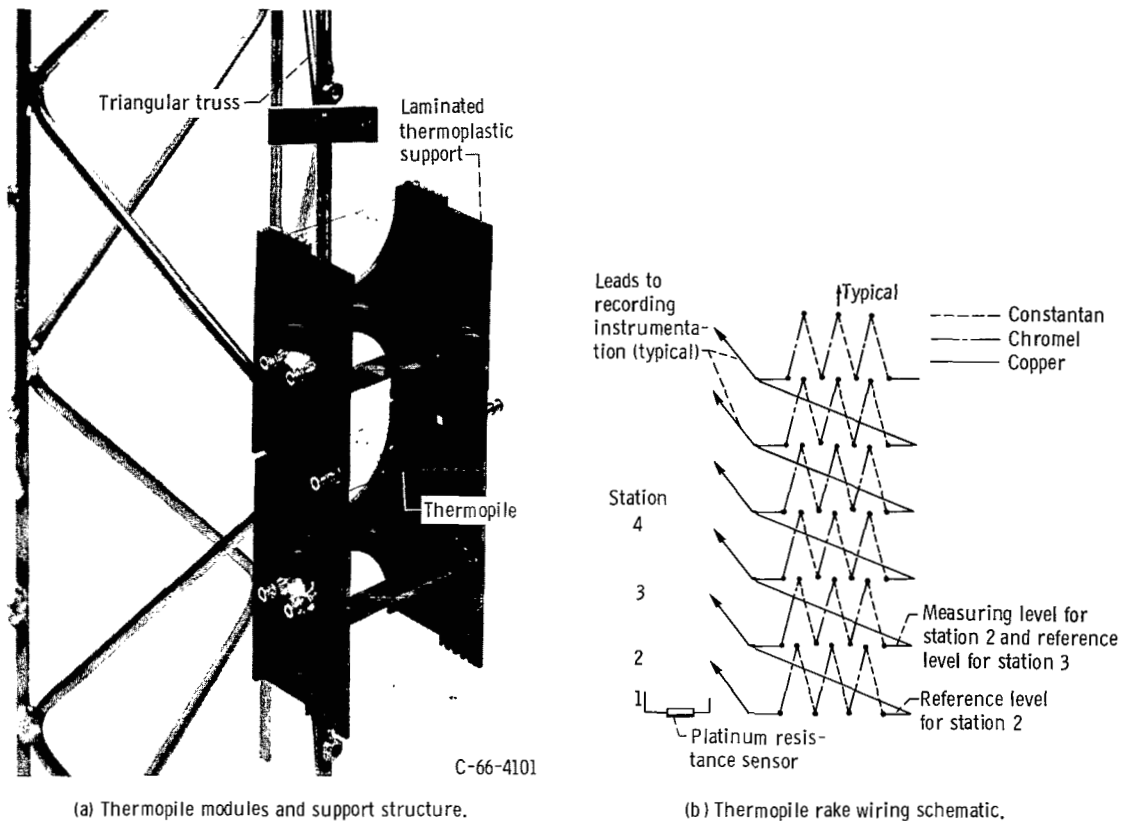


Figure 6. - Thermopile rake.

Platinum resistance sensors, which were located at least every tenth station starting from the bottom of the rake, sensed the absolute temperature at their location and provided a reference for the thermopiles above the location. The horizontal rakes were composed of platinum resistance sensors spaced a maximum of 33.0 centimeters (13.0 in.) apart in the radial direction. Two platinum resistance sensors were used at each location to measure liquid temperatures in the 20 to 38.9 K (36° to 70° R) range and gas temperatures in the 38.9 to 227.8 K (70° to 500° R) range. These dual sensors permitted more accurate measurement of both liquid and gas temperatures than could be achieved with one sensor covering the entire range.

The initial static temperature profile near the liquid surface was determined by an interface rake (fig. 5). This rake contained 17 platinum resistance sensors spaced 1.10 centimeters (0.43 in.) apart and hot-wire liquid level sensors spaced 0.64 centimeter (0.25 in.) apart. The range of the temperature sensors was 20 to 38.9 K (36° to 70° R). The initial liquid level was determined by the location of the saturation temperature (corresponding to tank pressure) on the interface rake and verified by means of liquid level sensors.

Platinum resistance sensors were also used to determine tank wall temperatures at 18 locations (every 10° starting from the bottom of the tank) and the liquid temperature at the flowmeter. Copper-constantan thermocouples were used to determine tank lid temperatures at five locations and the pressurant gas inlet temperature.

Concentrations. - The concentration of helium and hydrogen gas at five positions in the tank (fig. 5) was obtained by a gas sampling and analyzer system. A general schematic of this system is shown in figure 7. The sampling tubes had 0.157-centimeter- (0.062-in. -) outside diameters with a wall thickness of 0.030 centimeter (0.012 in.). To prevent liquid from entering the sampling tubes, a small helium gas purge was maintained in the tubes that were initially submerged in the liquid hydrogen.

The operation of a typical sampling tube is as follows: After the liquid passes the entrance of the sampling tube (during expulsion), the helium purge is stopped. The tank pressure then forces the gas sample through the tube to a flow regulator which maintains a flow of 35 cubic centimeters per minute into a mixing chamber. In the mixing chamber, the gas sample is mixed with 100 percent hydrogen which enters the chamber at a rate of 15 cubic centimeters per minute (the biasing of the gas sample enables the analyzer to operate in its most sensitive range). The biased gas sample then enters the analyzer at a rate of 50 cubic centimeters per minute. The analyzer then compared the thermal conductivity of the biased gas sample with that of 100 percent helium (the helium also enters the analyzer at 50 cm³/min). The output of the analyzer was continuously

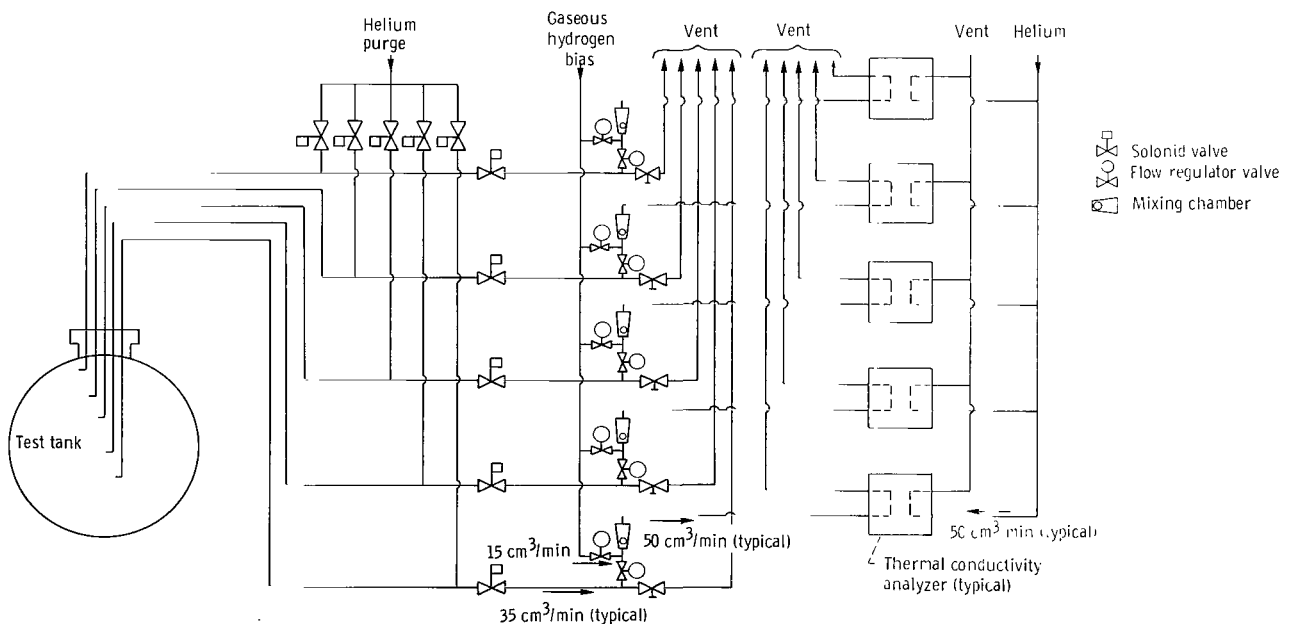


Figure 7. - Ullage gas sampler and analyzer system schematic.

recorded on a direct reading oscillograph. The helium and hydrogen gas concentration was then obtained by comparing the analyzer output with the output previously obtained when using known sample concentrations.

PROCEDURE

The spherical test tank was filled from the bottom to approximately a 2-percent ullage condition. It was then topped off as necessary while the tank lid and peripheral support hardware reached steady-state temperatures.

Temperature conditioning of the pressurant inlet line was then started. Gas flow was established through the heat exchanger loop, through the control valves and orifice arrangement, and then into the tank ullage from where it was vented to the outside as shown in figure 2. The temperature control circuit shown in figure 2 was used to get the desired pressurant gas temperature level during the flow period. When the pressurant gas temperature conditioning was almost completed, the liquid level in the test tank was adjusted to a desired value by either topping or slow draining. The pressurant gas flow was then stopped, and the test tank was vented in preparation for an expulsion run. The liquid level was determined from liquid level sensors on the interface rake. The automatic controllers and timers were preset with all the desired run and operating conditions (i. e., tank pressure level, length of ramp period, length of hold period, liquid outflow valve position, start and stop times of the data recording equipment, etc.).

After starting the data recording equipment, the next step of the completely automatic run sequence took electrical calibrations on all pressure transducers. Immediately following this, the test tank was pressurized over a predetermined time period to the nominal operating pressure of 34.47×10^4 newtons per square meter (50 psia). Tank pressure was held constant for about 30 seconds to stabilize internal temperatures. The tank expulsion period was then started. Approximately 90 percent of the total tank volume was expelled at a constant volumetric flow rate. The expulsion period was stopped when a hot-wire liquid level sensor located at the 95-percent ullage level indicated passage of the liquid interface. The last step of the automatic run sequence was the stopping of all data recording equipment. The test tank was then vented and refilled with liquid hydrogen for the next expulsion.

Ramp pressurization runs, with no expulsion, were made for four different tank ullage levels. The only deviation in the operating procedure for these runs was that the liquid outflow valve was locked shut.

DATA REDUCTION

The data reduction procedure used in this report is essentially the same as that used in reference 6. The complete data reduction procedure is presented in appendix D. The relations derived in appendix D that are used in the presentation of experimental results are now summarized.

Pressurant Gas Added (M_G)

The actual pressurant gas added to the tank ullage was determined from the relation

$$M_{G, i \rightarrow f} = \int_{t_i}^{t_f} YD^2 C \sqrt{\rho \Delta P^*} dt \quad (1)$$

Ideal Pressurant Requirement (M_I)

This report uses two different relations to define the ideal pressurant requirement. One is used to determine the ideal requirement for the initial pressurization of the tank and is given by

$$M_I = \frac{\bar{M} P_o V_o}{Z R T_G} \left[\left(\frac{P_f}{P_o} \right)^{1/\gamma} - 1 \right] \quad (2)$$

This expression assumes a one-component ullage. It also assumes that the pressurizing gas does not mix or exchange heat with the gas in the ullage volume. For the tests conducted herein, the initial ullage volume contained a mixture of hydrogen and helium. However, because of the method used to precondition the inlet gas temperature (described in the PROCEDURE section), the initial ullage volume was predominantly helium. Therefore, the ideal pressurant requirement used in this report is based on a 100 percent helium ullage (i. e., $\bar{M} = 4.003$, $\gamma = 1.67$). The ideal requirement that was used in references 4 and 5 is based on 100 percent hydrogen (i. e., $\bar{M} = 2.016$, $\gamma = 1.40$). In any case, the ideal requirement is just used as a normalizing factor and does not necessarily indicate a true minimum requirement.

The other relation, which is used to determine the ideal requirement during the expulsion period, is given by

$$M_I = \frac{\bar{M}P \Delta V_U}{ZRT_G} \quad (3)$$

The assumption used in obtaining this relation is that the incoming pressurant does not exchange heat or mass with the surroundings.

Energy Balance

Applying the first law of thermodynamics to the entire tank system (tank + ullage gas + liquid) results in the expression

$$\underbrace{\int_{t_i}^{t_f} [\dot{M}_G h_G + \dot{Q}] dt}_{\text{Total Energy Added } (\Delta U_T)} = \underbrace{\int_{t_i}^{t_f} [\dot{M}_L h_L dt + dU_L]}_{\text{Total change in liquid in tank + liquid expelled energy } (\Delta U_L)} + \underbrace{\int_{t_i}^{t_f} dU_U}_{\text{Total change in energy } (\Delta U_U)} + \underbrace{\int_{t_i}^{t_f} dU_W}_{\text{Total change in wall energy } (\Delta U_W)} \quad (4)$$

dividing through by ΔU_T gives

$$1 = \frac{\Delta U_L}{\Delta U_T} + \frac{\Delta U_U}{\Delta U_T} + \frac{\Delta U_W}{\Delta U_T} \quad (5)$$

These ratios show the relative distribution of the total energy input into the system. The data presented herein are in the form of these ratios.

Error Analysis

An analysis was performed to determine the magnitude of probable error which could be present in the integration of equations (4), (13), and (14) of appendix D. Prob-

TABLE I. - GAS MASS BALANCE RESULTS

[Hemisphere injector; tank pressure, $34.47 \times 10^4 \text{ N/m}^2$.]

| Run | Inlet gas temperature, K | Ramp time, sec | Hold time, sec | Expulsion time, sec | Tank cycle time, sec | Ramp | | | | Expulsion | | | | | | | | | |
|-----|--------------------------|----------------|----------------|---------------------|----------------------|-------------------------|----------------------------|----------------------------------|----------------------------|----------------------------|----------------------------------|-----------------------------|--------------|-----------|------------|------------------------------------|------------|-----------------------|-----------|
| | | | | | | Initial ullage mass, kg | Mass added during ramp, kg | Mass transferred during ramp, kg | Hold period | | | Mass added during expulsion | | | | Mass transferred during expulsion, | | Final ullage mass, kg | |
| | | | | | | | | | Ullage mass after ramp, kg | Mass added during hold, kg | Mass transferred during hold, kg | Ullage mass after hold, kg | Experimental | | Analytical | | M_t , kg | | M_t/M_G |
| | | | | | | | | | | | | | M_G , kg | M_I/M_G | M_G , kg | M_I/M_G | | | |
| 4 | 170 | 22.7 | 31.0 | 477.9 | 531.6 | 1.54 | 0.92 | 0.17 | 2.29 | 0.56 | 0.10 | 2.75 | 50.09 | 0.536 | 51.64 | 0.519 | 2.50 | 0.050 | 50.34 |
| 6 | 162 | 22.7 | 31.0 | 759.9 | 813.6 | 1.43 | .89 | .11 | 2.21 | .57 | .11 | 2.67 | 51.94 | .549 | 57.50 | .496 | 1.34 | .026 | 53.27 |
| 7 | 171 | 23.0 | 30.8 | 1119.3 | 1173.1 | 1.23 | .93 | -.38 | 2.55 | .64 | .22 | 2.97 | 56.17 | .485 | 61.13 | .445 | .19 | .003 | 58.95 |
| 12 | 303 | 21.4 | 31.9 | 983.9 | 1037.2 | 1.14 | .59 | .10 | 1.63 | .57 | .21 | 1.99 | 48.13 | .323 | 49.01 | .317 | 1.27 | .026 | 48.85 |
| 13 | 299 | 21.6 | 31.6 | 730.7 | 783.9 | 1.04 | .61 | -.41 | 2.06 | .60 | .31 | 2.35 | 45.12 | .349 | 45.52 | .345 | 3.27 | .072 | 44.20 |
| 15 | 301 | 21.5 | 31.7 | 456.1 | 509.3 | 1.08 | .63 | -.31 | 2.01 | .64 | .30 | 2.35 | 40.33 | .387 | 41.73 | .374 | 4.61 | .114 | 38.07 |

^aProbable error associated with each value is ± 0.02 kg.

TABLE II. - ENERGY BALANCE RESULTS

| Run | Inlet gas temperature, K | Expulsion time, sec | Expulsion | | | | | | | | | | | | |
|-----|--------------------------|---------------------|--|------------|--------------------------------|----------------------------|------------------|-------------------------|------------------|-------------------------|------------------|---|------------------|-------------------------|-------|
| | | | Energy added by pressurant gas, J | | Energy added by environment, J | Energy gained by tank wall | | | | Energy gained by ullage | | Energy gained by liquid | | | |
| | | | | | | Experimental | | Analytical | | | | Experimental | | Analytical | |
| | | | Experimental | Analytical | ΔU_w , J | $\Delta U_w/\Delta U_T$ | ΔU_w , J | $\Delta U_w/\Delta U_T$ | ΔU_U , J | $\Delta U_U/\Delta U_T$ | ΔU_L , J | $\Delta U_L/\Delta U_T$ | ΔU_L , J | $\Delta U_L/\Delta U_T$ | |
| 4 | 170 | 477.9 | ^a 450.6±0.1×10 ⁵ | 457.5 | 23.5×10 ⁵ | 193.2×10 ⁵ | 0.407 | 158.4×10 ⁵ | 0.329 | 149.4×10 ⁵ | 0.315 | ^a 112.3±16.9×10 ⁵ | 0.237 | 50.6 | 0.105 |
| 6 | 162 | 759.9 | 458.0±0.1 | 507.2 | 37.4 | 220.5 | .445 | 177.4 | .326 | 158.7 | .320 | 64.5±16.1 | .130 | 79.6 | .146 |
| 7 | 171 | 1119.3 | 506.1±0.2 | 551.1 | 55.0 | 249.4 | .444 | 206.6 | .341 | 156.4 | .279 | 49.2±19.7 | .088 | 118.1 | .195 |
| 12 | 303 | 983.9 | 760.6±0.2 | 775.0 | 48.4 | 499.8 | .618 | 437.6 | .531 | 157.8 | .195 | 112.8±17.0 | .139 | 104.5 | .127 |
| 13 | 299 | 730.7 | 709.4±0.2 | 716.1 | 35.9 | 456.7 | .613 | 391.8 | .521 | 159.5 | .214 | 77.9±22.2 | .104 | 77.5 | .103 |
| 15 | 301 | 456.1 | 639.3±0.2 | 661.7 | 22.4 | 369.9 | .559 | 314.8 | .460 | 169.1 | .256 | 96.7±18.3 | .146 | 48.2 | .070 |

^a ± Values show probable error associated with each measurement (absolute value).

able error is defined as follows: There is a 50-percent probability that the error will be no larger than the value stated. This analysis considered the errors introduced by the inaccuracies of temperature transducers as well as the tank pressure sensor. These calculations were performed for all runs for the expulsion period. The results of this analysis are included with the tabular data in tables I and II. No error analysis was performed on parameters which were dependent on the measured gas concentration data. The actual uncertainty of determining the gas concentration was unknown although it was estimated to be less than ± 20 percent.

RESULTS AND DISCUSSION

The main parameter used to compare the effectiveness of the various operating parameters on the amount of pressurant gas used is the nondimensional ratio M_I/M_G , where M_I is defined as the ideal helium pressurant mass required to pressurize or expel a given volume of liquid at a given inlet gas temperature and tank pressure with no heat or mass transfer, and M_G is the actual pressurant requirement for the same conditions. The ratio M_I/M_G could vary between 0 and 1. A high M_I/M_G ratio means less energy and mass exchange. It does not necessarily mean a low absolute pressurant requirement M_G as is illustrated later in this section.

A value of M_I/M_G equal to unity implies that there is no heat transferred to the tank wall or liquid and no mass transfer. This means that for no environmental heating, the terms $\Delta U_w/\Delta U_T$ and $\Delta U_L/\Delta U_T$ in equation (5) are zero and that $\Delta U_U/\Delta U_T$ is equal to one; that is, all the energy (ΔU_T) added to the tank during expulsion appears as an increase in ullage energy (ΔU_U). Therefore, any value of M_I/M_G or $\Delta U_U/\Delta U_T$ less than unity means energy is lost by the ullage system. This loss of ullage energy would then appear as a change in tank wall energy and/or liquid energy, that is, $\Delta U_w/\Delta U_T$ and/or $\Delta U_L/\Delta U_T$ would be greater than zero.

The discussion of results will first present the effects of the various operating parameters on the ratio M_I/M_G , only for the expulsion period which was of primary interest, followed by mass transfer M_T/M_G results. Then the results of the energy balances will be presented in an attempt to point out major reason for the ratios M_I/M_G or $\Delta U_U/\Delta U_T$ being less than one. Finally, a comparison will be made between the experimental results and the analytically predicted results to determine the validity of the analytical program. The analytical results are presented in the figures along with the corresponding experimental results. The comparison between experimental and analytical results will be given in terms of an average deviation. Average deviation is defined as

$$\frac{1}{\bar{N}} \sum \left[\frac{|(\text{Experimental ratio}) - (\text{Analytical ratio})|}{(\text{Experimental ratio})} \right] 100$$

where \bar{N} is the number of data points for a given set of operating conditions (i. e., for a constant inlet gas temperature of 300 K (540° R), \bar{N} would be 3 for the data presented in fig. 8). For convenience, all deviations between the experimental and analytical results are summarized in table III.

The operating parameters (e. g., inlet gas temperature and outflow rate, major experimental and analytical results) are summarized in tables I and II. Table I gives experimental and analytical mass balance results, and table II gives the corresponding energy balance results.

Effect of Inlet Gas Temperature and Expulsion Time

Pressurant requirements. - The effect of inlet gas temperature is shown in figure 8 on the basis of M_I/M_G for various expulsion times. Expulsion time is the total time required to expel liquid from a 5- to a 95-percent ullage. Therefore, each data point represents a complete expulsion. As may be seen in the figure, for a given inlet gas temperature, there is an increasing pressurant requirement (decreasing M_I/M_G) for increasing expulsion times. The longer the pressurant (ullage) gas is exposed to cold

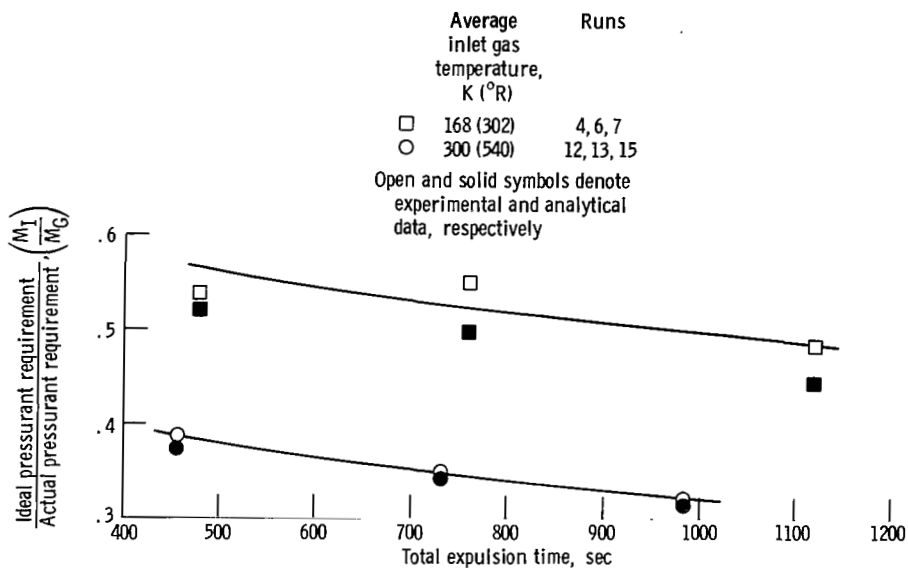


Figure 8. - Comparison of ideal pressurant requirement to actual pressurant requirement ratio as function of expulsion time for two inlet gas temperatures. Hemisphere injector; tank pressure, 34.47×10^4 newtons per square meter (50 psia).

TABLE III. - DEVIATIONS BETWEEN EXPERIMENTAL AND ANALYTICAL RESULTS
FOR THE EXPULSION PERIOD

| Run | Inlet gas temperature, K | Percent deviation between experimental and analytical results ^a | | |
|-----|--------------------------|--|-------------------------|-------------------------|
| | | M_I/M_G | $\Delta U_w/\Delta U_T$ | $\Delta U_L/\Delta U_T$ |
| 4 | 170 | +3.17 | +19.1 | +55.7 |
| 6 | 162 | +9.65 | +26.8 | -12.3 |
| 7 | 171 | +8.25 | +23.2 | -121.8 |
| 12 | 303 | +1.85 | +14.1 | +8.6 |
| 13 | 299 | +1.15 | +15.0 | + .9 |
| 15 | 301 | +3.36 | +17.7 | +52.0 |

^a+ Underprediction; - overprediction.

surroundings, the greater the loss in pressurant energy. Also, the ratio M_I/M_G decreases for increased inlet gas temperature (from a maximum of 0.550 for 168 K (302.4° R) to a minimum of 0.324 for the 300 K (540° R) inlet temperature). This implies that a larger percentage of energy contained in the pressurant gas is lost to the tank wall and liquid as the inlet gas temperature is increased. The values of M_I/M_G obtained here using helium as the pressurant are approximately 8.3 percent lower than those obtained in reference 5 using hydrogen as the pressurant for similar inlet gas temperature and expulsion times.

The lower values of M_I/M_G when using helium are believed to be the result of different modes of mass transfer for the two pressurant gases. Reference 5 indicated that the net mass transfer was evaporation, which in effect reduces the actual pressurant requirements M_G (or increases the M_I/M_G ratio) over that which would be required if there were no mass transfer. This report indicates, as will be discussed later, helium being absorbed in the liquid hydrogen. The absorption of helium increases the actual pressurant requirement M_G (decreases the M_I/M_G ratio) over the no mass transfer case.

A comparison of the actual pressurant requirements (M_G) for the two inlet gas temperatures for various expulsion times is shown in figure 9. The actual pressurant requirements (M_G) decrease for increased inlet gas temperature and increase for increasing expulsion times. There is an average decrease of 1.0 percent in pressurant gas requirements (M_G) for a 10 K (18° R) increase inlet gas temperature. The results of reference 5 indicated that there was an average decrease in pressurant gas requirements of 1.3 percent for a 10 K (18° R) increase in inlet gas temperature when using hydrogen as the pressurant gas. The actual pressurant mass required when using helium is ap-

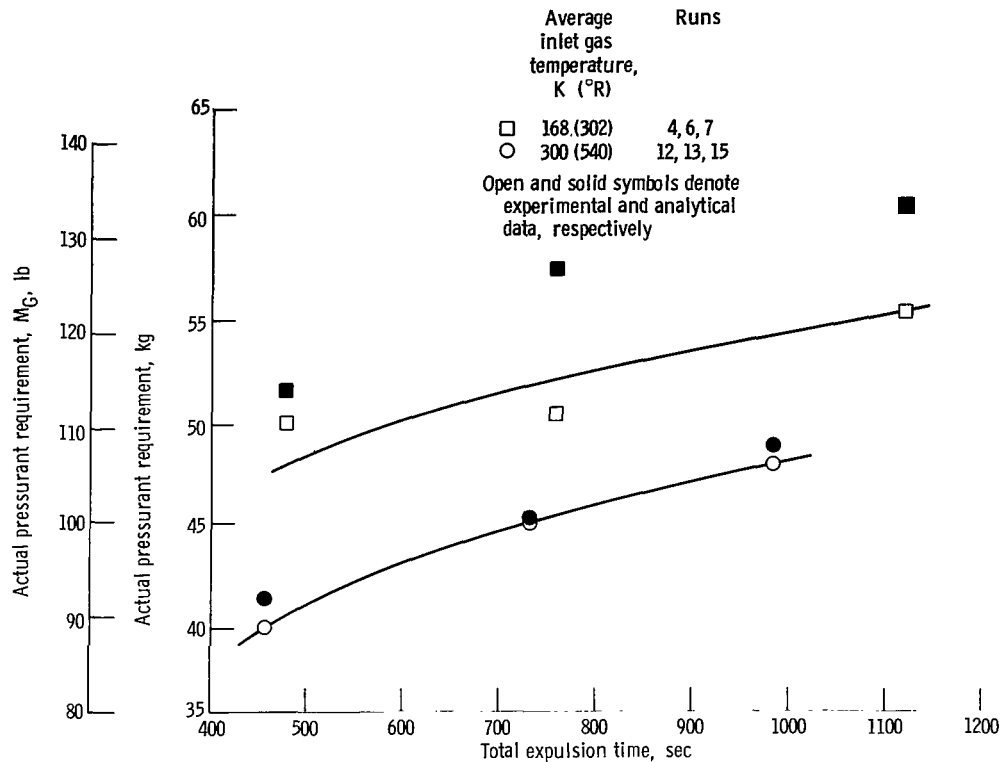


Figure 9. - Comparison of actual pressurant requirement as function of expulsion time for two inlet gas temperatures. Hemisphere injector; tank pressure, 34.47×10^4 newtons per square meter (50 psia).

proximately twice that required when using hydrogen as the pressurant for the same operating conditions. Although the absolute value of M_G decreases for increasing inlet gas temperatures, the ratio M_I/M_G at 300 K (540° R) is less than the M_I/M_G at 168 K (302.4° R) due to the greater decrease in ideal requirements.

The solid symbols in figures 8 and 9 are the results as predicted by the analytical program. The agreement is good between the analysis and experimental results for the 300 K (540° R) inlet gas temperature (see table III for actual deviations) and not as good for the 168 K (302.4° R) inlet temperature. The reason for the greater deviation for the lower temperature is not clearly understood. However, in all cases, the actual deviation is less than 10 percent.

As stated in the INTRODUCTION, another objective of the work described herein was to determine possible scale effects due to tank size. Figure 10 compares the mass ratio M_I/M_G just presented at an inlet gas temperature of 300 K (540° R) with that obtained in reference 6 using gaseous helium as the pressurant in a 1.52-meter- (5-ft-) diameter spherical tank for an inlet gas temperature of 322 K (580° R) over a wide range of expulsion times. As can be seen in the figure, the range of M_I/M_G values is not significantly different for the two tank sizes. The mass ratio ranges from 0.335 to 0.261

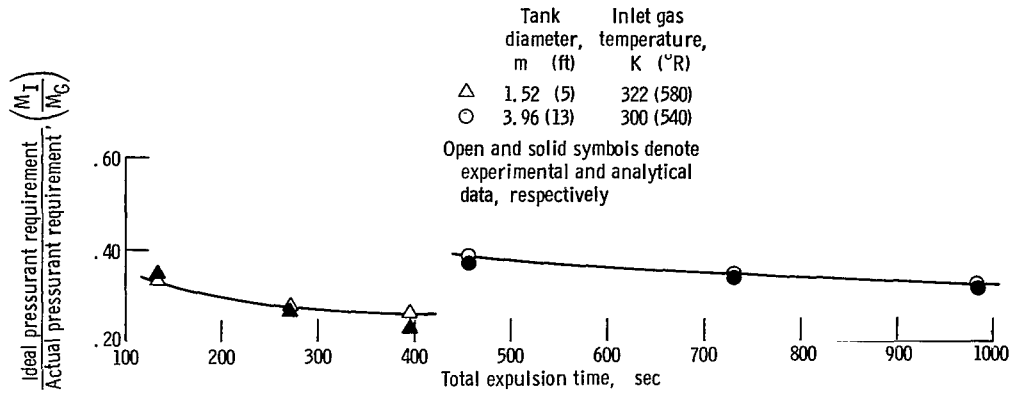


Figure 10. - Comparison of ideal pressurant requirement to actual pressurant requirement as function of expulsion time for two spherical tank sizes. Tank pressure, 34.47×10^4 newtons per square meter (50 psia); pressurant gas, helium.

for the 1.52-meter- (5-ft-) diameter tank and from 0.385 to 0.324 for the 3.96-meter- (13-ft-) diameter tank. The agreement would be even closer if either tank values were corrected for the 22 K (40° R) difference in inlet gas temperature.

Since the tank wall was shown to be the major heat sink of the tank system (refs. 3 to 6), it appears that a possible scaling parameter could be the rate at which the wall surface area is exposed to the ullage gas during the expulsion period ($A_{w,f} - A_{w,i}/\Delta t$). If $(A_{w,f} - A_{w,i})/\Delta t$ is used as a scaling parameter, a 135-second expulsion in the 1.52-meter- (5-ft-) diameter tank can be compared with a 915-second expulsion in the 3.96-meter- (13-ft-) diameter tank. The mass ratio values at these expulsion times are 0.335 and 0.330 for the 1.52- and 3.96-meter- (5- and 13-ft-) diameter tanks, respectively, which indicates that $(A_{w,f} - A_{w,i})/\Delta t$ could be a reasonable scaling factor, at least as far as pressurant gas requirements are concerned.

The agreement between the analytical (solid symbols in fig. 10) and experimental mass ratio values is good for both tank sizes, which also indicates that tank size can be accurately accounted for in the prediction of pressurant gas requirements.

Mass transfer. - The amount of mass transfer was not directly measured experimentally. It was determined indirectly by the use of equation (D8). The accuracy of determining the mass transfer is strongly influenced by the accuracy with which the gas sampling and analysis system determined the helium-hydrogen concentrations in the ullage.

A comparison of the ratio of mass transferred during expulsion to the actual pressurant added to the tank (M_t/M_G) is presented in figure 11 for different expulsion times and the two inlet gas temperatures. The experimental results presented in this figure indicate that helium is absorbed into the liquid hydrogen in all cases. There is a decreasing M_t/M_G ratio for increasing expulsion times; that is, there is decreased ab-

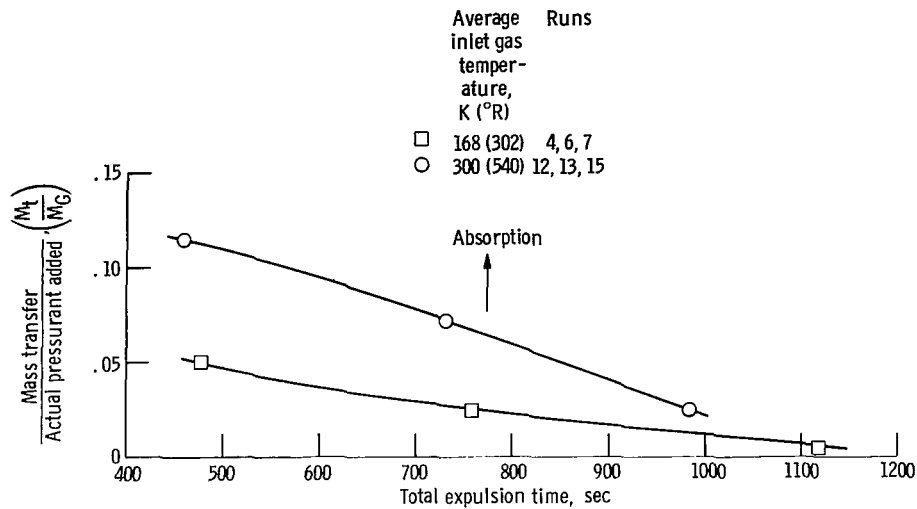


Figure 11. - Comparison of mass transfer to actual pressurant required ratio as function of expulsion time for two inlet gas temperatures; hemisphere injector; tank pressure, 34.47×10^4 newtons per square meter (50 psia).

sorption and a trend toward evaporation as expulsion time is increased (absolute values of M_t presented in table I).

As mentioned previously, the determination of mass transfer is strongly influenced by the determination of the helium-hydrogen gas concentration in the ullage. Figure 12 presents a typical ullage gas concentration profile prior to and after a 478-second expulsion. The percent hydrogen as a function of height relation (to the point where the ullage is 100 percent helium) is approximately the same prior to and after expulsion (i. e., from 0 to 0.51 m (0 to 1.67 ft) prior to expulsion and from 2.92 to 3.43 m (9.58 to 11.25 ft) after expulsion). However, the volume associated with the latter is larger resulting in a net increase of hydrogen gas in the ullage at the end of the expulsion period. This fact alone indicates evaporation and/or diffusion, but the use of equation (D8) for this run (run 4) resulted in a net value of mass transfer (absorption) of 2.50 kilograms (5.53 lb). Based on a 1.2-mole-percent solubility of helium in liquid hydrogen (ref. 8), the maximum amount of helium that could go into solution (into 2150 kg (4740 lb) of liquid hydrogen) is approximately 51.6 kilograms (113.8 lb). Even though all absorption values were well below this maximum value the actual mass-transfer values are not considered reliable because of the uncertainties in determining the concentration gradients.

There are no analytical comparisons for the mass transfer because the analysis neglects mass transfer in the development.

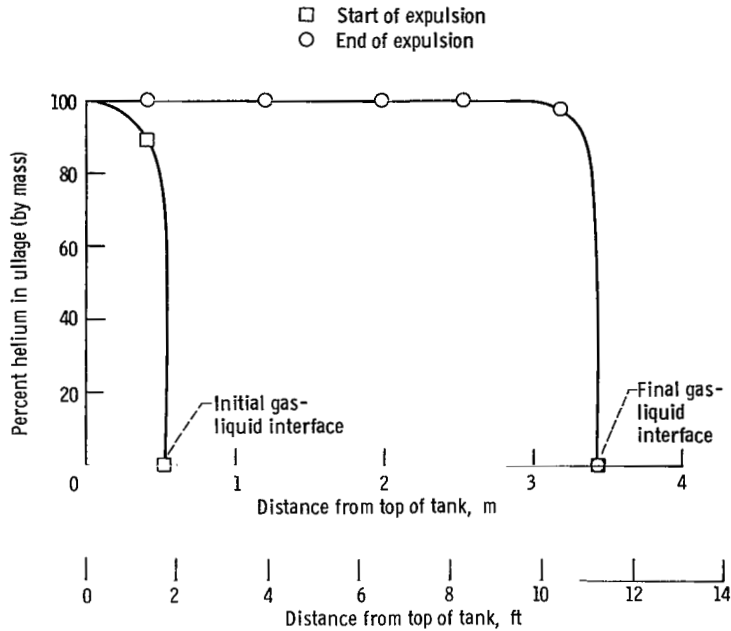


Figure 12. - Typical ullage gas concentration profile before and after expulsion. Inlet gas temperature, 170 K (306° R); tank pressure, 34.47×10^4 newtons per square meter (50 psia).

Energy Remaining in Ullage

The ratios of the energy increase in the ullage over the expulsion period to the total energy added to the system $\Delta U_U / \Delta U_T$ for different expulsion times are compared in figure 13 for the two inlet gas temperatures. For all runs, between 19.5 and 32.0 percent of the total energy that was added to the system remains in the ullage after expulsion. For any given expulsion time, the ratio $\Delta U_U / \Delta U_T$ decreases for increasing inlet gas temperatures. Also, for a given inlet gas temperature, the ratio $\Delta U_U / \Delta U_T$ decreases with increasing expulsion time. It should be noted that the absolute value of ΔU_U does not change significantly for the two operating inlet gas temperatures used during testing. The mean increase in ullage energy for these series of runs (table II) was 1584.7×10^4 joules (15 021 Btu) with a standard deviation of 63.5×10^4 joules (602 Btu). Any trends in the ratio $\Delta U_U / \Delta U_T$, therefore, depend mainly on variations in the total energy added (ΔU_T) to the system due to variations in energy losses to the tank wall and liquid.

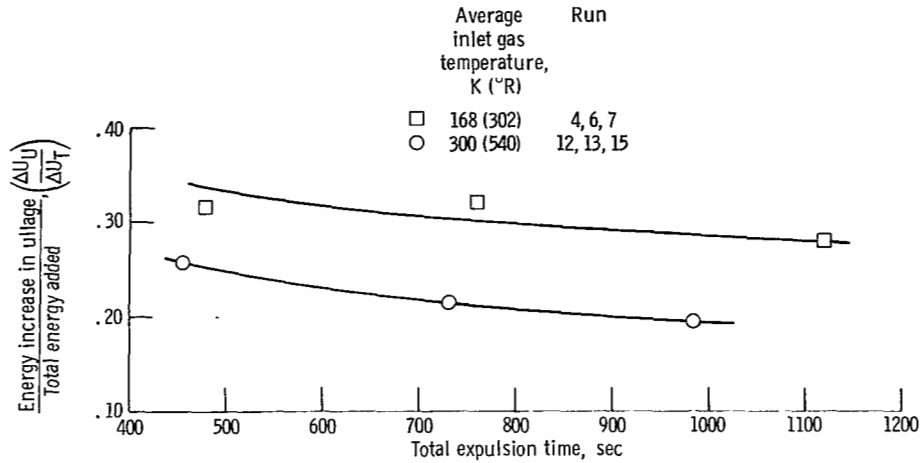


Figure 13. - Comparison of energy increase in ullage to total energy added ratio as function of expulsion time for two inlet gas temperatures. Hemisphere injector; tank pressure, 34.47×10^4 newtons per square meter (50 psia).

Energy Added to Tank Wall

The ratio of energy gained by the tank wall to the total energy added to the system ($\Delta U_W / \Delta U_T$) for different expulsion times are compared in figure 14 for the two inlet gas temperatures. In general, between 40.5 and 62.0 percent of the total energy added to the system was gained by the tank wall over the range of conditions. The results of reference 5 showed that between 35.9 and 57.9 percent of the total energy added to the tank was gained by the tank wall for similar test conditions when using hydrogen as the pressurant. A comparison of results indicate that there is generally a 7- to 12.7-percent increase in the fraction of total energy that is lost to the tank wall ($\Delta U_W / \Delta U_T$) when using helium as the pressurant. The absolute values for wall energy gain (ΔU_W) were actually less when using helium as the pressurant (probably the result of the lower heat-transfer coefficient for helium compared with hydrogen under the same operating conditions). However, the decrease in total energy added (ΔU_T) when using helium is even greater because of its lower specific heat, resulting in the increase of the $\Delta U_W / \Delta U_T$ ratio over that obtained when using hydrogen. As may be seen in table II and in figure 14, both the absolute value of ΔU_W and the ratio $\Delta U_W / \Delta U_T$ increase with increasing inlet gas temperature. The increase in ΔU_W is due to the larger driving potential (ΔT) for heat transfer between the ullage gas and the tank wall. The total energy added to the system (ΔU_T) does not increase in the same proportion as ΔU_W resulting in the increased ratio $\Delta U_W / \Delta U_T$.

The agreement between the analytical and experimental value of $\Delta U_W / \Delta U_T$ is poor. The analysis underpredicts the $\Delta U_W / \Delta U_T$ ratio by averages of 23.0 and 15.9 percent for the 168 and 300 K (302.4° and 540° R) inlet gas temperatures, respectively.

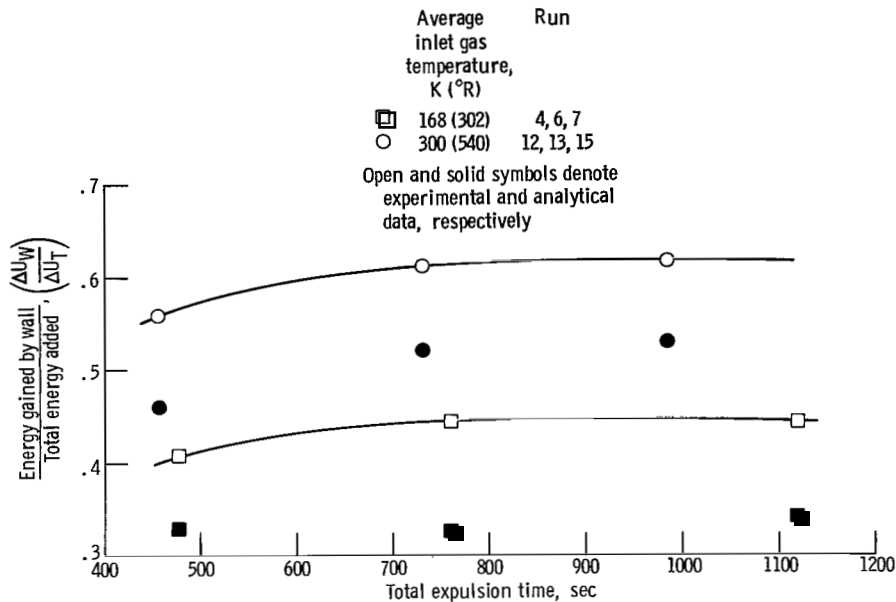


Figure 14. - Comparison of energy gained by wall to total energy added ratio as function of expulsion time for two inlet gas temperatures. Hemisphere injector; tank pressure, 34.47×10^4 newtons per square meter (50 psia).

Energy Gained by Liquid

Figure 15 is a comparison of the ratio of energy gained by the liquid to the total energy added to the system ($\Delta U_L / \Delta U_T$) for different expulsion times for the two inlet gas temperatures. In all cases between 8.8 and 23.7 percent of the total energy added to the system appears as an increase in liquid energy (liquid heating). The results of reference 5 indicate that between 12.8 and 33.7 percent of the total energy added to the system appear as an increase in liquid energy for similar test conditions using hydrogen as the pressurant. With the exception of the 984-second run with an inlet gas temperature of 300 K (540° R), the data indicate a decreased $\Delta U_L / \Delta U_T$ ratio for increasing expulsion times and for increased inlet gas temperature. However, the probable error associated with each experimental determination of ΔU_L is between 15 and 40 percent (see table II). Therefore, no reliable conclusions can be drawn from these particular data.

The analytical predictions of the ratio $\Delta U_L / \Delta U_T$ are also presented in figure 15 (see table III for average deviations). The large discrepancy between the analysis and experimental results could also be the result of the error in determining ΔU_L .

A composite of the energy distributions just presented for the 300 K (540° R) inlet gas temperature in the 3.96-meter - (13-ft-) diameter tank is compared in figure 16 with that obtained in reference 6 using a 1.52-meter - (5-ft-) diameter spherical tank over a

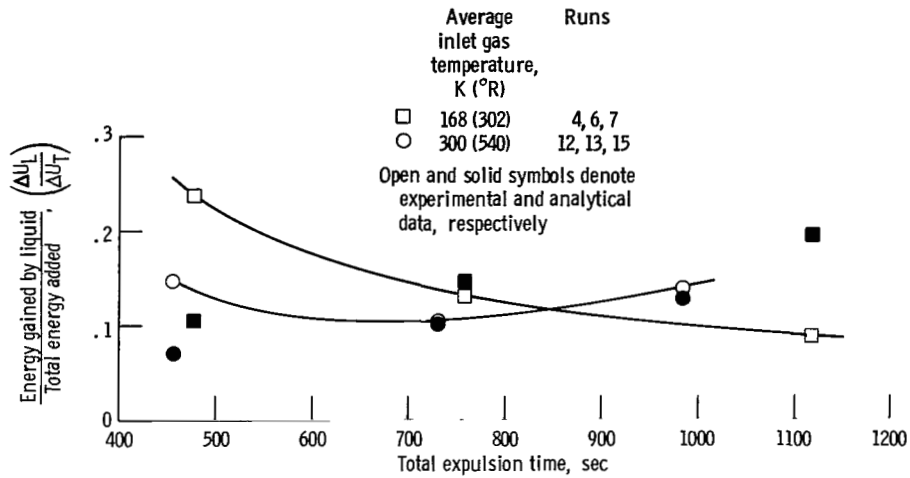


Figure 15. - Comparison of energy gained by liquid to total energy added ratio as function of expulsion time for two inlet gas temperatures. Hemisphere injector; tank pressure, 34.47×10^4 newtons per square meter (50 psia).

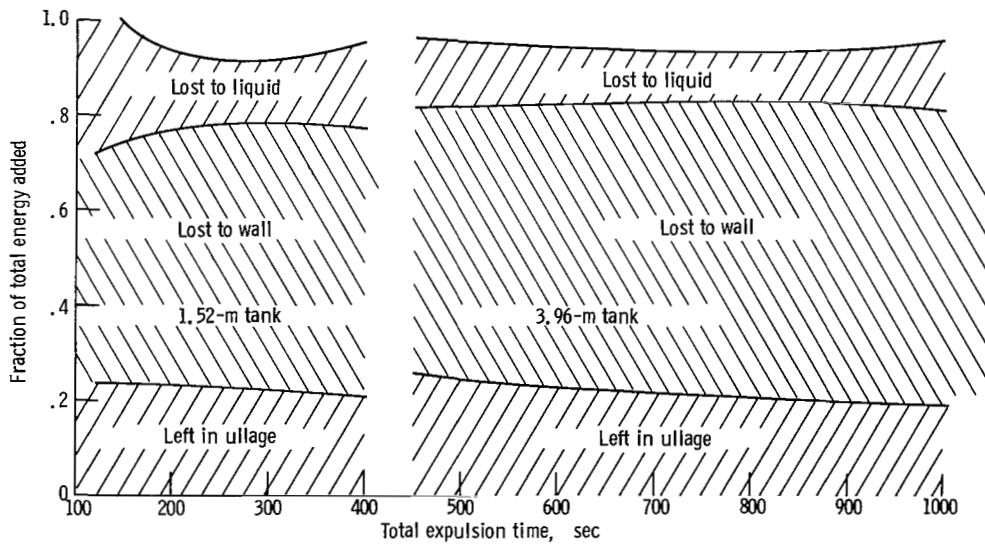


Figure 16. - Comparison of energy distribution at end of expulsion for two spherical tank sizes as function of expulsion. 1.52-Meter (5-ft) tank: inlet gas temperature, 322 K (580° R); tank pressure, 34.47×10^4 newtons per square meter (50 psia). 3.96-Meter (13-ft) diameter tank: inlet gas temperature, 300 K (540° R); tank pressure, 34.47 newtons per square meter (50 psia).

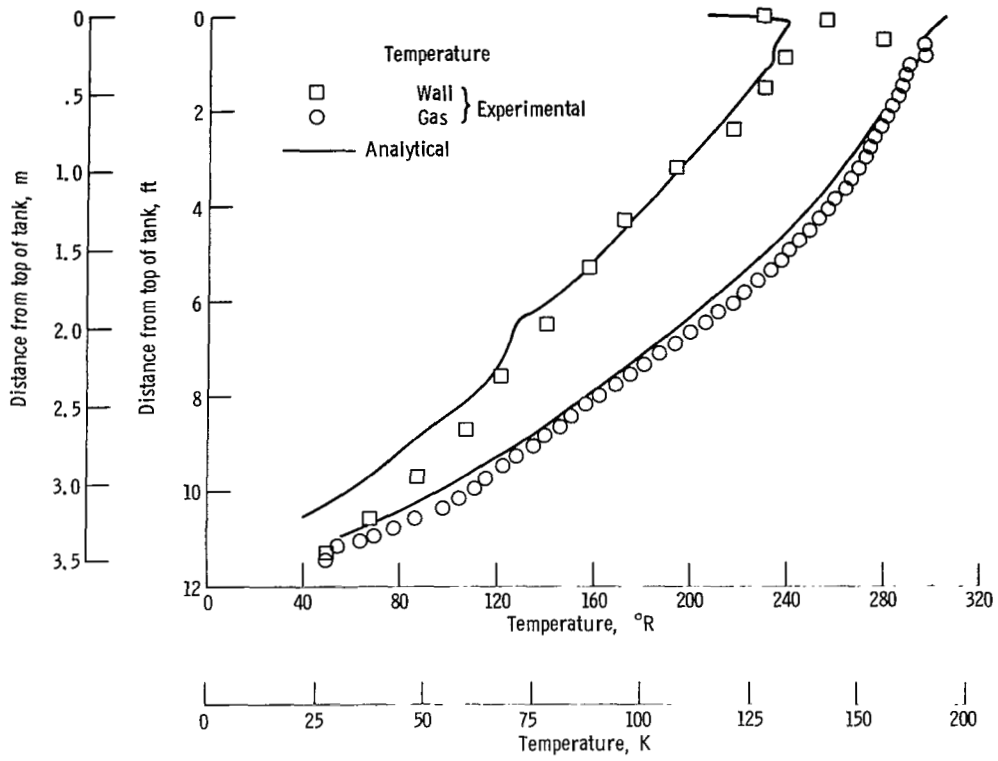
range of expulsion times. The inlet gas temperature for the 1.52-meter- (5-ft-) tank was 322 K (580° R). The final energy distributions for the two tank sizes are very similar. The tank wall in both cases represents the major heat sink of the tank system. Between 50 and 63 percent of the total energy added to the tank system is absorbed by the tank wall. Between 19.5 and 25 percent remains in the ullage and the remainder is either absorbed by the liquid or is unaccounted for (due to instrumentation uncertainties). Tank size then, for these operating conditions, does not greatly influence the energy distribution in the system at the end of expulsion.

Temperature Distribution

The results that were discussed previously point out that between 72.2 and 82.7 percent of the total energy that was added to the system is either absorbed by the tank wall or remains in the ullage for the 3.96-meter- (13-ft-) diameter tank. The correlation between the analysis and experimental data, therefore, depends largely on the ability of the analysis to predict final wall and ullage gas temperature profiles. These profiles are, in turn, used to determine the increase in wall and ullage energy and the final ullage mass. The ability to predict these temperatures was used to explain the fair agreement between experimental data and analyses reported in references 1 and 3 to 5.

Figure 17 presents a comparison of experimental and analytical ullage gas and wall temperature profiles for the present investigation. These data are for a run (run 4) for which the values of the deviations between the experimentally and analytically determined ratios M_I/M_G and $\Delta U_w/\Delta U_T$ was near the mean of all the runs (see table III). The experimental gas temperatures shown in figure 17 were obtained from the vertical rake. The horizontal rakes indicated that these are the average radial temperatures at their respective vertical positions. In the absence of any mass transfer, the pressurant mass required for an expulsion could be determined as the difference between the final mass in the ullage and the initial mass in the ullage prior to expulsion.

One of the inputs to the analytical program is the initial experimental temperature profile prior to expulsion. The analytical program uses the profile together with the temperature-density relation for helium to obtain the initial ullage mass. The initial ullage mass as determined by the analysis is, in all cases, larger than determined experimentally because the experimental values include the binary gas. However, the difference between the analytically and experimentally determined initial ullage mass represents only a small fraction (less than 2 percent) of the final ullage mass. Therefore, the deviation between the analytical and experimental pressurant requirements would largely be the result of the predicted final ullage gas temperature profile. As can be seen in figure 17, the analytical gas temperatures are slightly lower through-



out the ullage volume. As a result, the predicted final ullage mass is slightly higher leading to an underprediction of the M_I/M_G ratio by 3.17 percent.

The analytically predicted wall temperatures (fig. 17) are generally lower than those observed experimentally, especially in the lower half and upper quarter of the tank. As a result, the energy gained by the tank wall determined analytically is less than that determined experimentally leading to an underprediction of the $\Delta U_w/\Delta U_T$ ratio by 19.1 percent.

Pressurant Requirements for Initial Pressurization

The amount of pressurant gas needed to initially pressurize a propellant tank may be important for certain mission, particularly for multiburn missions where the tank is vented after each burn or where the coast period between firings is long enough to enable the ullage gas to collapse.

As stated in the INTRODUCTION, the purpose of this investigation was to determine the capability of the analysis to predict the pressurant requirements during the initial pressurization period as well as the expulsion period. For this purpose, data were collected during the initial pressurization period for various pressurizing rates, inlet gas temperatures and ullage volumes.

Figure 18 is a comparison of the M_I/M_G ratio as a function of inlet gas temperature for two ramp rates at an initial ullage volume of approximately 5 percent. The data were taken using the hemisphere injector. At constant inlet gas temperature, the pressurant requirements decreased (M_I/M_G increased) for increased ramp rates. The M_I/M_G ratio decreases for increasing inlet gas temperature at constant ramp rates.

The modification of the analysis of reference 1 for the ramp period is discussed in appendix C. As can be seen in figure 18, the analysis is not capable of accurately predicting the pressurant requirements during the initial pressurization of the 5-percent ullage. However, the prediction of the total pressurant requirement (initial pressurization and expulsion) is still good because the amount of gas required to initially pressurize the 5-percent ullage was only 2.0 percent (maximum) of the pressurant requirement during expulsion. The absolute pressurant requirements (both experimental and analytical) for the data presented in figures 18 and 19 are given in table IV.

The comparison of M_I/M_G as a function of initial ullage volume for a ramp rate of 2.48×10^3 newtons per square meter per second (0.36 psi/sec) at an inlet gas temperature of approximately 165 K (297° R) is shown in figure 19. The M_I/M_G ratio at the 28-percent ullage is much higher than that indicated for the other initial ullage volumes. During this particular ramp run, there was a great deal of liquid evaporation. Of the total mass added to the ullage volume during this ramp, approximately 22 percent was

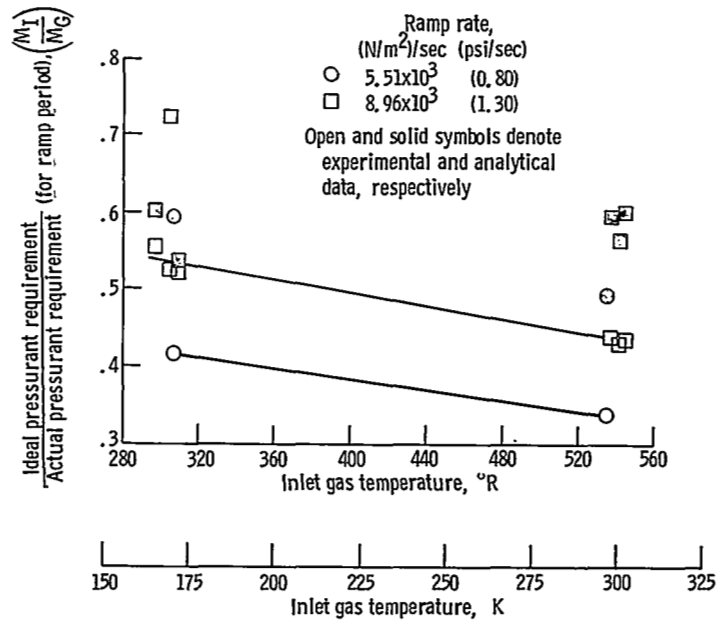


Figure 18. - Comparison of ideal pressurant requirement to actual pressurant requirement ratio for the ramp period as function of inlet gas temperature for two ramp rates. Ullage volume, 5 percent.

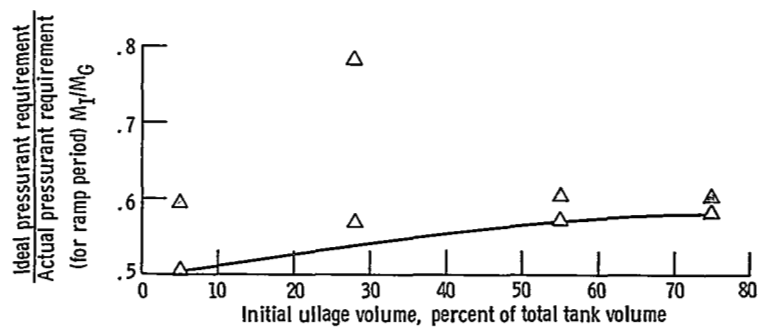


Figure 19. - Ideal pressurant requirement to actual pressurant requirement ratio as function of initial ullage volume for a ramp rate of 2.48x10³ newtons per square meter per second (0.36 psi/sec). Inlet gas temperature, 165 K (297° R).

TABLE IV. - COMPARISON OF EXPERIMENTAL AND ANALYTICAL VALUES OF
PRESSURANT GAS REQUIREMENTS FOR THE RAMP PERIOD

| Run | Initial ullage volume, percent | Ramp rate | | Inlet gas temperature | | Mass added experimental | | Mass added analytical | | M_I/M_G | |
|-----|--------------------------------|--------------------|---------|-----------------------|-------------|-------------------------|-------|-----------------------|-------|-------------|------------|
| | | $N/(m^2)(sec)$ | psi/sec | K | $^{\circ}R$ | kg | lb | kg | lb | Experiments | Analytical |
| | | | | | | | | | | | |
| 2 | 5 | 5.51×10^3 | 0.80 | 170.6 | 307 | 1.18 | 2.60 | 0.83 | 1.82 | 0.416 | 0.594 |
| 3 | | 2.48 | .36 | 165 | 297 | .94 | 2.08 | .78 | 1.71 | .505 | .594 |
| 4 | | 8.96 | 1.30 | 171.7 | 309 | .92 | 2.02 | .89 | 1.97 | .519 | .534 |
| 6 | | 8.96 | 1.30 | 165.6 | 298 | .89 | 1.96 | .82 | 1.81 | .554 | .600 |
| 7 | | 8.96 | 1.30 | 169.4 | 305 | .93 | 2.06 | .68 | 1.50 | .523 | .720 |
| 10 | | 5.51 | .80 | 297.8 | 536 | .81 | 1.78 | .55 | 1.22 | .338 | .491 |
| 12 | | 8.96 | 1.30 | 302.8 | 545 | .59 | 1.30 | .43 | .94 | .435 | .600 |
| 13 | | 8.96 | 1.30 | 298.3 | 537 | .61 | 1.35 | .45 | .99 | .437 | .594 |
| 15 | | 8.96 | 1.30 | 301.1 | 542 | .63 | 1.38 | .48 | 1.05 | .430 | .562 |
| 66 | 28 | 2.48 | .36 | 165.6 | 298 | 3.19 | 7.04 | 3.66 | 8.07 | .783 | .570 |
| 79 | 55 | 2.48 | .36 | 164.4 | 296 | 8.27 | 18.23 | 8.07 | 17.80 | .571 | .604 |
| 94 | 75 | 2.48 | .36 | 162.8 | 293 | 11.91 | 26.26 | 11.50 | 25.35 | .582 | .603 |

due to liquid evaporation. The evaporation of liquid reduced the actual pressurant requirement resulting in the high value of M_I/M_G . The reason for the large amount of evaporation for this particular run is not known. If this data point is ignored, the remaining data indicate increased M_I/M_G for increased ullage volume. Here again, the analysis is not capable of accurately predicting the pressurant requirements. However, the analytical predictions improve for the larger ullage volumes. The transient process that occurs during the initial pressurization of the tank is too complex to be described by the present analytical model, particularly for small ullages. The analytical program can, however, at least be used to predict the approximate magnitude of pressurant requirements during the ramp period.

SUMMARY OF RESULTS

Tank pressurization and propellant expulsion tests were conducted in a 3.96-meter- (13-ft-) diameter spherical tank to (1) determine what factors have the greatest influence on pressurant gas requirements when using helium as the pressurant during the expulsion of liquid hydrogen, (2) compare these results with those obtained in references 5 and 6, and (3) verify the capability of an analysis to predict the helium pressurant requirements during the initial pressurization period as well as the expulsion period.

Tests were conducted using a hemisphere injector for two inlet gas temperatures over a range of liquid outflow rates. The results of this investigation are the following:

1. The experimental results indicate an average decrease in helium pressurant gas requirements of 1.0 percent for a 10 K (18⁰ R) increase in inlet gas temperature in the range covered.

2. Increased inlet gas temperature decreased the residual mass and the fraction of the total energy that remains in the ullage volume after expulsion. The decrease in the fraction of the total energy remaining in the ullage is due to an increase in the fractions that were lost to the tank wall and liquid. Of the total energy added to the tank system between 40.5 and 62.0 percent was lost to the tank wall and between 8.8 and 23.7 percent was lost to the liquid.

3. The mass transfer values obtained in this investigation are inconclusive due to the uncertainty in measuring the ullage gas concentration gradients. However, the experimental results indicated absorption in all cases. The amount of absorption decreased for increased inlet gas temperature and increased expulsion time. Additional work is necessary to develop better techniques for measuring gas concentration gradients and mass transfer.

4. The effect of inlet gas temperature and ramp rate on the pressurant gas required during the initial pressurization of the tank were as follows:

(a) Increasing the inlet gas temperature decreased the pressurant requirement (M_G) and mass ratio (M_I/M_G) for constant ramp rates.

(b) Increasing the ramp rate decreased the pressurant requirement and increased the mass ratio for constant inlet gas temperatures.

(c) For a constant ramp rate, the pressurant requirements and mass ratio increased for the larger initial ullage volumes.

5. The trends shown in this report for various inlet gas temperatures and liquid outflow rates are consistent with the results obtained using hydrogen as the pressurant (ref. 5). A comparison of the results obtained for the two pressurants indicate that the mass ratio M_I/M_G for similar test conditions for helium is an average of 8.3 percent lower than for hydrogen. It, therefore, would require more than twice as much mass to expel liquid hydrogen using helium as the pressurant than if hydrogen were used.

6. The trends shown in this report are also consistent with the results obtained in a 1.52-meter- (5-ft-) diameter spherical tank (ref. 6) indicating that the scale effects due to the tank size are predictable.

The comparison between the analytical and experimental results indicate that, for the range of test conditions used, the analytical program and assumptions are adequate to allow prediction of the pressurant gas requirements during the initial pressurization as well as the expulsion period when using helium as the pressurant. The general results as predicted by the analysis were as follows:

1. The pressurant mass requirements were predicted to within an average of 2.1 percent for the 300 K (540° R) inlet gas temperature and within 7.0 percent for the 168 K (302.4° R) inlet gas temperature.
2. Tank wall heating was predicted to within an average of 19.3 percent for all runs.
3. The prediction of liquid heating was not good. The average deviation from experimental values was 41.9 percent. Additional refinements to the analysis are needed to improve the prediction of liquid heating. However, this poor prediction of liquid heating (under the conditions imposed herein) does not hamper the ability to accurately predict the pressurant requirements.

Lewis Research Center,
National Aeronautics and Space Administration,
Cleveland, Ohio, August 10, 1970,
180-31.

APPENDIX A

VARIABLE GEOMETRY, HEAT LOSS TO TANK WALL, AND INTERNAL HARDWARE

The basic analysis used in this report for predicting pressurant gas requirements was developed by W. H. Roudebush in reference 1 for a cylindrical tank.

The major assumptions in the analysis of reference 1 are as follows:

- (1) The ullage gas is nonviscous.
- (2) The ullage gas velocity is parallel to the tank axis and does not vary radially or circumferentially.
- (3) The tank pressure does not vary spatially.
- (4) The ullage gas temperature does not vary radially or circumferentially.
- (5) The tank wall temperature does not vary radially or circumferentially.
- (6) There is no axial heat conduction in either the gas or the wall.
- (7) There is no mass transfer (condensation or evaporation).
- (8) There is no heat transfer from the pressurant gas to the liquid.

Experiments performed at Lewis (ref. 3) confirmed most of these assumptions when using a diffuser type of injector such as the one used in this report. The experimental results indicated, however, that there is significant heat transfer from the gas to the liquid with resulting mass transfer.

For the purposes of this report, the analysis of reference 1 was modified for application to arbitrary symmetric tank shapes, and an attempt was made to incorporate the heat transfer from the gas to the liquid. The treatment of internal hardware (e. g. , tank baffles, and instrumentation) was also modified to correspond to the treatment of heat transfer to the tank wall.

The primary equations that deal with the pressurizing gas on entering the tank are

- (1) The energy equation
- (2) The continuity equation
- (3) The tank-wall heat transfer
- (4) The heat and mass transfer at the gas-liquid interface.

Energy Equation

The form of the energy equation used in the analysis in reference 1 for cylindrical tanks is

$$\frac{\partial T}{\partial t} = \frac{2h_c ZRT}{rMPC_p} (T_w - T) - \bar{V} \frac{\partial T}{\partial x} + \frac{RTZ_1}{MPC_p} \frac{\partial P}{\partial t} + \frac{RTZ\dot{q}_H C_H}{\pi r^2 MPC_p}$$

Modifying this equation to account for both arbitrary, symmetric tank shapes and internal tank heat sinks gives

$$\frac{\partial T}{\partial t} = \frac{2h_c ZRT}{rMPC_p} (T_w - T) \left[1 + \left(\frac{dr}{dx} \right)^2 \right]^{1/2} - \frac{\bar{V}}{\partial x} \frac{\partial T}{\partial x} + \frac{RTZ_1}{MPC_p} \frac{\partial P}{\partial t} + \frac{\dot{Q}_H}{C_p M_H} \quad (A1)$$

The first term on the right includes the effect of wall curvature. The last term, the energy lost to the internal hardware, is treated as the summation of hardware components: (1) laminated thermoplastic, (2) stainless steel, and (3) copper. For the tanks in this investigation,

$$\frac{\dot{Q}_H}{M_H} = \sum_{\substack{\text{Hardware} \\ \text{components}}} \frac{A_H h_c (T_H - T_G)}{\rho_H V_H} \quad (A2)$$

Gluck and Kline (ref. 6) employed the free convection correlation to the pressurant gas (hydrogen, helium) for the pressurized transfer of liquid hydrogen:

$$\frac{h_c L}{k} = Nu = 0.13(GrPr)^{1/3} \quad (A3)$$

This correlation is used herein even though it was developed for cylindrical tanks. Pressurant gas transport properties were evaluated at the mean of the gas and wall temperatures.

Continuity Equation (Area = f(x))

The basic form of the continuity equation for a cylindrical tank is presented in reference 1 (eq. (24)) as

$$\frac{\partial \bar{V}}{\partial x} = \frac{Z_1}{ZT} \left(\frac{\partial T}{\partial t} + \bar{V} \frac{\partial T}{\partial x} \right) - \frac{Z_2}{ZP} \frac{\partial P}{\partial t}$$

The modified form of the continuity equation, because of variations in tank radius with distance along the vertical axis, becomes

$$\frac{\partial \bar{V}}{\partial x} = \frac{Z_1}{ZT} \left(\frac{\partial T}{\partial t} + \frac{\bar{V}}{\partial x} \frac{\partial T}{\partial x} \right) - \frac{Z_2}{ZP} \frac{\partial P}{\partial t} - \frac{2\bar{V}}{r} \frac{\partial r}{\partial x} \quad (\text{A4})$$

where Z_1 and Z_2 are defined in reference 1 as

$$Z_1 \equiv Z + T \left(\frac{\partial Z}{\partial T} \right)_P$$

$$Z_2 \equiv Z - P \left(\frac{\partial Z}{\partial P} \right)_T$$

The last term in equation (A4) evolves from the following derivation for the one-dimensional expression for continuity:

$$\frac{\partial}{\partial x} (\rho \bar{V} A) + \frac{\partial}{\partial t} (\rho A) = 0$$

The substitution $A = \pi r^2$ is made where r is the position radius at location x along the vertical axis:

$$\frac{\partial}{\partial x} (\rho \bar{V} r^2) + \frac{\partial}{\partial t} (\rho r^2) = 0$$

The expression for density from the equation of state $\rho = \bar{M}P/ZRT$ is substituted:

$$P \frac{\partial}{\partial x} \left(\frac{\bar{V} r^2}{ZT} \right) + r^2 \frac{\partial}{\partial t} \left(\frac{P}{ZT} \right) = 0$$

The following velocity equation is obtained after performing the partial differentiation and after rearranging terms:

$$\frac{\partial \bar{V}}{\partial x} = \left[\frac{1}{T} + \frac{1}{Z} \left(\frac{\partial Z}{\partial T} \right)_P \right] \left(\frac{\partial T}{\partial t} + \frac{\bar{V}}{\partial x} \frac{\partial T}{\partial x} \right) + \left[\frac{1}{Z} \left(\frac{\partial Z}{\partial P} \right)_T - \frac{1}{P} \right] \frac{\partial P}{\partial t} - \frac{2\bar{V}}{r} \frac{\partial r}{\partial x}$$

When the expressions involving Z_1 and Z_2 are substituted in this equation, equation (A4) is obtained.

Tank Wall Heat Transfer

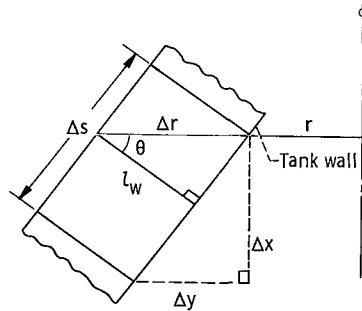
Reference 1 (eq. (18)) gives the heat-transfer equation that represents the change in wall temperature as a result of the convective process for a cylindrical tank:

$$\frac{\partial T_w}{\partial t} = \frac{h_c}{l_w \rho_w C_w} (T - T_w) + \frac{\dot{q}_w}{l_w \rho_w C_w} \quad (\text{A5})$$

where \dot{q}_w is the rate of heat addition per unit area to the tank wall from outside the tank.

For a small element of volume in the x -direction, equation (A5) can be written as

$$\rho_w C_w V \frac{\partial T_w}{\partial t} = h_c A (T - T_w) + \dot{Q}_w \quad (\text{A6})$$



(a)

For a wall of arbitrary shape, the following is evident from sketch (a):

$$\frac{A}{V} = \frac{2\pi r \Delta s}{2\pi r \Delta r \Delta x} = \frac{\Delta s}{\Delta r \Delta x} = \frac{1}{l_w}$$

Therefore, equation (A5) holds also for this case.

To account for the large mass concentration at the top of the tank, an equivalent l_w was used. This l_w was obtained by dividing the mass of the tank lid and flange connection by the surface area at the first net point (fig. 20).

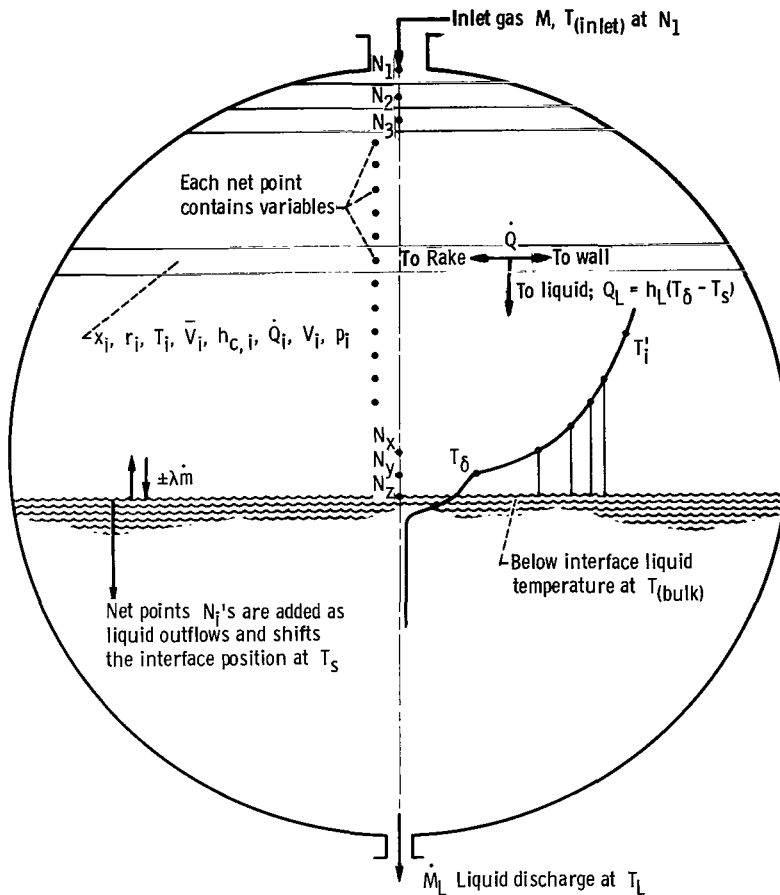


Figure 20. - Analytical model. Coordinate system is positive in the downward direction from $x = 0$ at N_1 to $x = n$ at the interface N_2 .

APPENDIX B

EQUATIONS OF HEAT AND MASS TRANSFER AT THE GAS-LIQUID INTERFACE

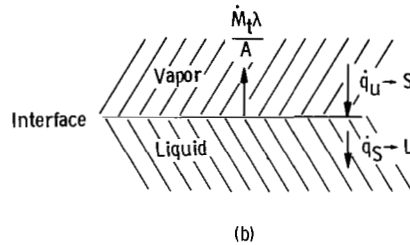
The energy and continuity equations (A1) and (A4) should be modified to incorporate both heat transfer from the ullage gas to the liquid surface and mass transfer into the analysis.

The energy equation should incorporate three additional terms:

- (1) The heat-transfer rate from the ullage gas to the liquid interface, $\dot{q}_{U \rightarrow S}$
- (2) The heat-transfer rate from the interface to the liquid, $\dot{q}_{S \rightarrow L}$
- (3) The energy $\dot{M}_t \lambda$ associated with mass transfer (evaporation is positive)

These additional terms can be related by performing an energy balance at the gas-liquid interface as done by W. A. Olsen in reference 10. The resulting energy relation is based on the assumption requiring the interface for a pure system to be at the saturation temperature corresponding to the tank pressure.

The energy balance at the interface is shown schematically in sketch (b):



It follows from sketch (b) that

$$\dot{q}_{U \rightarrow S} = \dot{q}_{S \rightarrow L} + \frac{\dot{M}_t \lambda}{A} \quad (B1)$$

In the case where helium is the pressurant gas for liquid hydrogen, it is assumed that there is sufficient evaporation to maintain a hydrogen blanket over the entire liquid surface. The interface can then be assumed to be at the saturation temperature for a pure hydrogen system.

The experimental data indicate that the energy associated with the mass transfer was relatively small, thus the following assumption is made:

$$\frac{\dot{M}_t \lambda}{A} \cong 0$$

With the further qualification that the environmental heat transfer to the liquid is also small, it follows that

$$\dot{q}_{U \rightarrow S} \cong \dot{q}_{S \rightarrow L} \cong \frac{d}{dt}(U_L) \quad (B2)$$

The term $d/dt(U_L)$ can be determined from experimental data. However, the analysis requires that $\dot{q}_{U \rightarrow S}$ be related to the ullage gas variables. This is done by the following equation, which involves defining a heat-transfer coefficient $h_{c, L}$ and a temperature T_δ somewhere in the vapor:

$$\dot{q}_{U \rightarrow S} \equiv h_{c, L}(T_\delta - T_{sat}) \quad (B3)$$

The flow process is free convection flow of pressurant gas essentially down the tank wall and then radially inward across the liquid surface.

With regard to $h_{c, L}$, in reference 11 an equation was developed from boundary-layer theory for forced flow across a horizontal, semi-infinite, constant-temperature flat plate given by

$$Nu = \frac{h_{c, L} L}{k} = 0.664 \left(\frac{\mu C_p}{k} \right)^{1/3} \left(\frac{L \bar{V}_L \rho}{\mu} \right)^{1/2} \quad (B4)$$

The velocity \bar{V}_L of the gas across the liquid surface, in terms of the gas velocity \bar{V}_G down a vertical wall, is given in reference 12 as

$$\bar{V}_L = 0.0975 \bar{V}_G \quad (B5)$$

where \bar{V}_G , obtained by solving the integrated energy and momentum equations at the wall boundary, is given by

$$\bar{V}_G = 1.185 \frac{\mu}{\rho Z} \frac{Gr^{1/2}}{\left[1 + 0.494(Pr)^{2/3} \right]^{1/2}} \quad (B6)$$

Combining equations (B5) and (B6) for \bar{V}_L and substituting into (B4) give

$$\text{Nu} = \frac{h_{c, L} L}{k} = \frac{0.226(\text{Pr})^{1/3}(\text{Gr})^{1/4}}{\left[1 + 0.494(\text{Pr})^{2/3}\right]^{1/4}} = 0.21(\text{Pr})^{1/3}(\text{Gr})^{1/4} \quad (\text{B7})$$

for a value of Pr between 0.74 and 0.90.

Equation (B7) is similar in form to the empirical relation for free convection flow along vertical planes and cylinders given in reference 13 as

$$\text{Nu} = \frac{h_{c, L} L}{k} = n(\text{GrPr})^m \quad (\text{B8})$$

Equation (B8) is used in this analysis (with $m = 1/3$ and $n = 0.14$) because it is simpler and it fits the data somewhat better than equation (B7).

At this point, some choice of T_δ , which is consistent with the definition of $h_{c, L}$ and fits the data for \dot{q}_{U-S} (i. e., $d/dt(U_L)$), must be made.

In reference 14 in which the experiment involved the pressurization of liquid hydrogen with a low mixing diffuser and no liquid outflow, the adiabatic compression temperature given by $T_{ad} = T_o(P/P_o)^{(\gamma-1)/\gamma}$ was used as the choice for T_δ . This relation gave good agreement between analytical and experimental mass flux results for the hydrogen pressurant. For the conditions described in reference 14, appreciable condensation occurred. Reference 14 indicated that as T_δ increases there is a tendency toward evaporation away from the condensation results that occurred when the adiabatic temperature was used. With ullage gas mixing (due to diffuser characteristics as well as the liquid outflow process), T_δ would be expected to be greater than T_{ad} .

For the work described herein, T_δ was obtained from the following relation evaluated with experimental data:

$$\dot{q}_{U-S} = h_{c, L}(T_\delta - T_{sat}) = \frac{d}{dt}(U_L)$$

One experimental run, where the expulsion time was 730 seconds (run 13), was used for the determination of T_δ where $h_{c, L}$ is given by equation (B8). For this condition, T_δ was determined to be 1.1 times the adiabatic compression temperature or 37.8 K (68° R) for a tank pressure of $34.47 \times 10^4 \text{ N/m}^2$ (50 psia). For convenience this value of T_δ was used for all comparisons since the effect of the interfacial terms in the energy equation was small in the experimental situation.

Using equation (B8) as well as the values for T_δ and T_{sat} result in the final form of the equation used to evaluate the heat transferred from the ullage gas to the liquid interface:

$$\dot{q}_{U \rightarrow S} = \frac{k}{L} (0.14)(GrPr)^{1/3} (T_{\delta} - T_{sat}) \quad (B9)$$

In order to incorporate liquid heating to the analysis, either

$$- \frac{\dot{q}_{U \rightarrow S} A_L}{X_n V \rho} \quad \text{or} \quad - \frac{k(0.14)(GrPr)^{1/3} (T_{\delta} - T_{sat}) A_L}{L X_n V \rho} \quad (B10)$$

must be added to the right side of equation (A1).

APPENDIX C

RAMP ANALYSIS

The amount of pressurant gas needed to initially pressurize a propellant tank may be important for multiburn missions. When the coast period between firings is long, a collapse in ullage pressure may develop. Under these circumstances a significant amount of pressurant may be necessary to repressurize the propellant tank for the next firing.

An application of the work reported in reference 1 is the prediction of the pressurant requirements for the initial pressurization (ramp) and hold periods. A separate computer program, which determines the pressurant as well as energy requirements during the ramp and hold periods, is described herein. The same equations that describe the expulsion period, as outlined in appendix A, are also applicable for the ramp and hold periods. However, the ramp period is more difficult to model analytically than the expulsion period, particularly for small ullage volumes where the liquid surface is near the injector outlet. Even though the experimental results indicated relatively large amounts of mass transfer during this period, the incorporation of mass transfer into the ramp analysis was not attempted because of the added complexity and incomplete knowledge of the mass-transfer phenomenon. The heat transfer from the ullage to the liquid surface is also neglected in the analytical model for the ramp period.

The analysis used for the ramp period computes the gas temperatures in the ullage at any time during the pressure rise from the gas energy equation. The corresponding gas velocities are computed from the equation of continuity. The iterative method to be described shows how convergence is achieved in the solution of the gas energy and continuity equations. The predicted mass of pressurant is based on an integration of the volume elements in the ullage at the end of the ramp and hold periods assuming a one-component ullage (100 percent helium). Quantitatively, the entire mass of pressurant requirements for the ramp period was less than the expulsion period by a factor of 30 to 60 when the initial ullage was 5 percent of the tank volume.

INPUT DATA REQUIREMENTS

For the solution to proceed, a set of boundary and initial conditions are required. These conditions, which are the same for the expulsion as well as the pressurization, are as follows:

- (1) At time $t = 0$, the values of gas temperature T and wall temperature T_w as functions of x

- (2) On the boundary $x = 0$, the value of inlet gas temperature T as a function of time
- (3) At the liquid surface, the value of gas temperature T , wall temperature T_w , and velocity \bar{V} as functions of time (Although movement of the interface has been noted during the ramp pressurization period, no significant effect on the programmed output was noted with the value of $\bar{V} = 0$ at the interface.)
- (4) Tank pressure P , outside heating rate \dot{q}_w , and inside hardware heating rate \dot{q}_H as functions of time (Like the other initial conditions, the pressure P as a function of time or ramp pressure curve is defined by a discrete set of points that approximate a smooth curve. In regions of pronounced curvature, more points are needed for accurate definition than for linear portions.)
- (5) Constant value of heat transfer coefficient h_c , or a correlating equation from which h_c may be evaluated at each net point from values of T , T_w , and P
- (6) Tank radius as a function of axial distance down from the top of the tank
- (7) Tank wall material properties: density ρ_w and specific heat $C_w(T_w)$
- (8) Tank wall thickness (average membrane plus weld area thickness) as a function of axial distance from the top of the tank
- (9) Pressurizing gas properties: Molecular weight \bar{M} , specific heat $C_p(T)$, and compressibility factor $Z(P, T)$
- (10) Initial ullage height, total time of run, number of net points in the initial ullage space
- (11) The initial time step Δt used in following the pressure rise as well as establishing the points of computation
- (12) If the hold period is to be included in the analysis, then the time for the end of the ramp must be specified

APPLICATION OF BASIC EQUATIONS

Reference 1 makes the substitution of $T_{w,i}$ from the finite difference form of (A6) into the finite difference form of the energy equation. Rearranging gives a quadratic in the gas temperature T'_i where the prime refers to a step forward in time and the quantities without the prime are evaluated at the previous time step:

$$T_i'^2 + \left[\alpha_i^* \left(1 + \bar{V}_i^* \frac{\Delta t}{\Delta x} - \omega_i^* \right) - T_{w,i} - \left(\frac{\dot{q}_w \Delta t}{l_w \rho_w C_w} \right)_i^* \right] T_i' - \alpha_i^* \left(\bar{V}_i^* \frac{\Delta t}{\Delta x} T_{i-1}' + T_i \right) = 0 \quad (C1)$$

The quantity marked with the asterisk may be evaluated either at the beginning or the end of the time interval.

A difficulty can arise when evaluating the gas energy equation expressed by the previous quadratic. This occurs when the heat transfer takes place from the wall into the ullage gas. For this situation, the solution of the continuity equation provided negative gas velocities, which made it impossible for equation (C1) to converge on the real roots.

At the start of the ramp (immediately after filling the tank), the initial wall temperature distribution in the ullage is higher than the gas temperature distribution. This is brought about because the wall surface above the liquid is exposed to the ambient temperature. But the ullage gas temperature near the liquid interface is close to the saturation temperature at 1 atmosphere.

The technique used when $T_{w,i} > T_i$ involved a direct substitution. The finite difference form of equation (A4) is

$$\bar{V}'_i = \frac{\left[T'_i \bar{V}'_{i+1} - \left(\frac{Z_1}{Z} \right)_i \left(\frac{\Delta x}{\Delta t} \right) (T'_i - T_i) + \left(\frac{Z_2}{Z} \right)'_i \frac{T'_i \Delta x}{P' \Delta t} (P' - P) \right]}{T'_i + \left(\frac{Z_1}{Z} \right)'_i (T'_{i+1} - T'_i) - 2 \frac{\Delta x}{r_i} T'_i \left(\frac{\Delta r}{\Delta x} \right)} \quad (C2)$$

Combining the equations involving ullage gas temperature T'_i and velocity \bar{V}'_i (eqs. (C1) and (C2)), the following cubic results:

$$\begin{aligned} b_i T_i'^3 + \left[\left(\frac{Z_1}{Z} \right)'_i T'_{i+1} + b_i c_i + \alpha_i^* \frac{\Delta t}{\Delta x} (\bar{V}'_{i+1} + d_i) \right] T_i'^2 + \left[c_i \left(\frac{Z_1}{Z} \right)'_i T'_{i+1} \right. \\ \left. + \alpha_i^* \frac{\Delta t}{\Delta x} \left(\frac{Z_1}{Z} \right)'_i \frac{\Delta x}{\Delta t} T_i - \alpha_i^* \frac{\Delta t}{\Delta x} T'_{i-1} (\bar{V}'_{i+1} + d_i) - \alpha_i^* T_i \frac{\Delta t}{\Delta x} b_i \right] T_i' \\ \left. - \alpha_i^* \frac{\Delta t}{\Delta x} \left(\frac{Z_1}{Z} \right)'_i \frac{\Delta x}{\Delta t} T_i T'_{i-1} - \alpha_i^* T_i \left(\frac{Z_1}{Z} \right)'_i T'_{i+1} = 0 \quad (C3) \end{aligned}$$

This arrangement of terms eliminates \bar{V}'_i , and the cubic is solved for the gas temperature T'_i .

ANALYTICAL PROCEDURE

The analytical procedure uses a variable time increment Δt in following the pressure rise. With this technique, the iteration was stable over a range of inlet conditions, and the results were consistent with the recorded data.

First, the velocity distribution is determined in the initial ullage at time $t = 0$. The substituted form of equation (A4) (in which the energy eq. (A1) is substituted for $\partial T/\partial t$) is put into finite difference form and solved for the velocity distribution for the first time.

For many of the ramp runs encountered in this investigation, an initial time increment of 1 second proved satisfactory.

Temperature Calculations from Top to Interface

Having obtained values of \bar{V} at each net point at time $t = t_1 = 0$, attention is turned to equation (C3) which is cubic in T'_i .

During the iteration, the cubic equation (C3) is solved for the gas temperature T'_i starting at the point N_2 in figure 20. When this equation is first solved for the ullage temperature distribution, a value for T'_{i+1} is not available. The value of T'_{i+1} was used as an initial guess for T'_{i+1} to get convergence. All other quantities in equation (C3) are available from the initial conditions. And the value for T'_{i-1} , the temperature at N_1 , is known as a boundary condition.

The solution for T'_i at N_3 follows, and this procedure continues to calculate gas temperatures until the boundary at the interface is reached. The values for the corresponding wall temperatures are calculated using the finite difference form of equation (A6).

VELOCITY CALCULATIONS FROM INTERFACE TO TOP

Although the ullage temperatures are computed starting at the top (fig. 20), the velocity equation (C2) is used to calculate the ullage gas velocity starting with the point N_y near the interface. The velocity at the interface N_z , the boundary value, is zero with no expulsion.

The ullage gas velocity is calculated from point to point until the top of the tank is reached. The new velocities are used in equation (C3) along with previous values of T'_{i+1} and the temperature distribution is redetermined. This process is continued until convergence is achieved over the entire ullage. The time is then advanced to t_2 and a new set of velocities is determined.

COMPLETING THE SOLUTION

With the new velocities at time t_2 , equation (C3) is evaluated again starting at point N_2 and terminating at the interface. A value for T'_{i+1} is always available from the previous iteration, although a substituted value of T'_{i+1} is used as the first value.

The new values for T'_i at all the points for time t_2 are used to recompute the velocity distribution. This new set of velocities is then compared with the previous set and convergence is assumed if the deviation is less than half of 1 percent for every velocity in the time set. A time step is then taken to t_3 .

If convergence is not achieved after 40 iterations, the time step is reduced, and the iteration process is reinitiated. Generally, the reduction in time step becomes necessary only when there is a severe change in the slope of the ramp curve, particularly in the early stages of the pressure rise (fig. 21).

For the new time t_3 , the temperature T'_i in equation (C3) is determined from its converged value using the iterative method. This procedure continues to evaluate the gas temperatures and velocity distribution in the ullage for each time step taken in following the rate of pressure in the tank.

The initial gas velocity distribution used in solving equation (C3) for each new time t is obtained from the previous time as follows:

$$V_{t, 2} = V_{t, 1} \frac{\frac{\Delta P_{1-2}}{\Delta t_{1-2}}}{\frac{\Delta P_{0-1}}{\Delta t_{0-1}}} \quad (C4)$$

This iterative procedure can be used for a constant pressure representing the hold period. However, for initiating the ramp, an actual pressure rise must be used. A typical example is shown in figure 21.

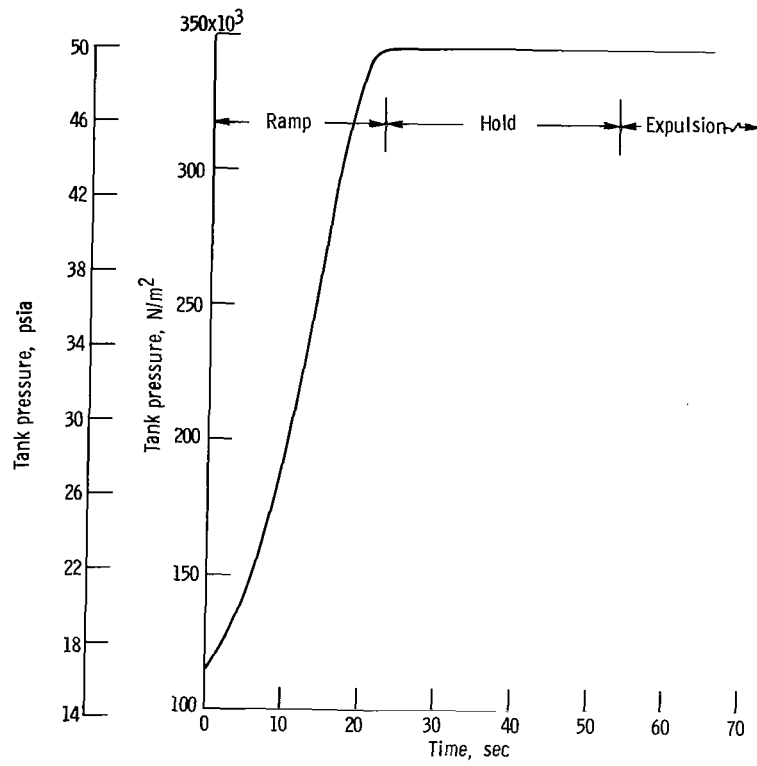


Figure 21. - Tank pressure as function of time during initial pressurization period for run 13.

APPENDIX D

DATA REDUCTION

PHYSICAL DESCRIPTION OF PROBLEM

An initially vented tank containing two-phase hydrogen was pressurized from 1 atmosphere to a new pressure by adding gaseous helium. The system was then allowed to stabilize at which time liquid outflow was started. During this expulsion period, pressurant gas (helium at constant temperature) was added to the tank at a rate that maintained a constant tank pressure while expelling the liquid at a desired rate. The amount of pressurant gas used during the expulsion phase is dependent on (1) the volume of liquid displaced with no heat or mass transfer, (2) the heat transfer to the tank wall and liquid, (3) the amount of mass condensed or evaporated, and (4) the amount of helium gas absorbed by the liquid hydrogen.

The main parameter used in the comparisons was the ratio of the ideal pressurant requirement to the actual pressurant requirement. The ideal pressurant was determined under the assumption that the incoming pressurant gas did not exchange energy or mass with the surroundings. Under this assumption, the ideal pressurant required for the initial pressurization of the tank was determined by the adiabatic relation

$$M_I = \frac{\bar{M} P_o V_o}{Z R T_G} \left[\left(\frac{P_f}{P_o} \right)^{1/\gamma} - 1 \right] \quad (D1)$$

The ideal pressurant required for the expulsion period was determined by the relation

$$M_I = \frac{\bar{M} P \Delta V_U}{Z R T_G} \quad (D2)$$

MASS BALANCE

A mass balance was performed on the ullage volume from an initial time t_i to a final time t_f as follows

$$M_{U,f} = M_{U,i} + M_{G,i \rightarrow f} \pm M_{t,i \rightarrow f} \quad (D3)$$

A discussion of how the terms of equation (D3) are determined appears in the next sections.

Pressurant Gas Added

The weight of the actual pressurant gas added from any initial time t_i to any final time t_f was determined by numerical integration of the gas orifice equation:

$$M_{G, i \rightarrow f} = \int_{t_i}^{t_f} YD^2C\sqrt{\rho \Delta P^*} dt \quad (D4)$$

Note that $(t_f - t_i)$ is the time necessary to expel ΔV_U of liquid.

Ullage Mass

The initial ullage mass $M_{U, i}$ and final ullage mass $M_{U, f}$ were obtained by numerical integration of the particular density profiles as follows:

$$M_{U, i} = \int_{V_{U, i}} \rho dV \approx \sum_{n=1}^{N_i} \rho_n V_n \quad \text{where } \rho = f(T, X_{H_2}, X_{He}) \quad (D5)$$

$$M_{U, f} = \int_{V_{U, f}} \rho dV \approx \sum_{n=1}^{N_f} \rho_n V_n \quad \text{where } \rho = f(T, X_{H_2}, X_{He}) \quad (D6)$$

The internal tank volume was considered as 57 (corresponding to thermopile location) horizontal disk segments. Each of these segments was in turn divided radially into a series of concentric rings, the number of which depended on location of radial temperature sensors and the vertical position of the disk segment being considered. These rings (339 in all) comprised the V_n 's in the calculations. In this manner, vertical temperatures as well as radial temperature gradients could be incorporated into the mass calculations. The position of the liquid level before and after expulsion determined the number of gas volume rings (N_i and N_f) used in the ullage mass calculations. The density of the two component ullage was calculated from the Beattie-Bridgeman equation of state for a mixture given in reference 15 as

$$P = \frac{RT(1 - \epsilon)}{\bar{M}'v^2} (v + B_T) - \frac{A_T}{v^2} \quad (D7)$$

where

$$A_T = \left(X_{H_2} \sqrt{A_{H_2}} + X_{He} \sqrt{A_{He}} \right)^2 \left(1 - \frac{X_{H_2} a_{H_2} + X_{He} a_{He}}{v} \right)$$

$$B_T = \left(X_{H_2} B_{H_2} + X_{He} B_{He} \right) \left(1 - \frac{X_{H_2} b_{H_2} + X_{He} b_{He}}{v} \right)$$

$$\epsilon = \frac{X_{H_2} C_{H_2} + X_{He} C_{He}}{vT^3}$$

Equation (D7) can then be solved for $1/v_n$ (where $1/v_n = \rho_n$) by knowing the pressure, temperature, and ullage gas concentration for each ΔV_n segment.

Mass Transfer

The mass transfer was calculated from equation (D3) as a result of knowing $M_{U,f}$, $M_{U,i}$, and $M_{G,i \rightarrow f}$, that is,

$$M_{t,i \rightarrow f} = M_{U,i} + M_{G,i \rightarrow f} - M_{U,f} \quad (D8)$$

If $M_{t,i \rightarrow f}$ was a positive quantity, mass was considered leaving the ullage volume (e. g., condensation and or absorption).

ENERGY BALANCE

For the thermodynamic system consisting of the entire tank and its contents (tank + ullage gas + liquid), the first law of thermodynamics for an increment of time dt may be written as

$$dU_T = (\delta M_G) \left(u_G + P_G v_G + \frac{\bar{V}_G^2}{2g} + z_G \right) - (\delta M_L) \left(u_L + P_L v_L + \frac{\bar{V}_L^2}{2g} + z_L \right) + \delta Q - \delta W \quad (D9)$$

The kinetic and potential energy terms are small in comparison with the other energy terms and will be neglected in this development. If $h = u + Pv$ is substituted, equation (D9) becomes

$$dU_T = (\delta M_G)h_G - (\delta M_L)h_L + \delta Q - \delta W \quad (D10)$$

For this system, there is no external work done on the system, so $\delta W = 0$; and the final form of equation (D9) becomes

$$dU_T = (\delta M_G)h_G - (\delta M_L)h_L + \delta Q \quad (D11)$$

Equation (D11) can be integrated over any time period. The physical interpretation of the quantities in equation (D11) is

$$\underbrace{\int_{U_i}^{U_f} dU_T}_{\substack{\text{Change in sys-} \\ \text{tem energy} \\ \text{(Tank + gas + liquid)}}} = \underbrace{\int_{t_i}^{t_f} \dot{M}_G h_G dt}_{\substack{\text{Energy input by} \\ \text{pressurant gas} \\ \text{inflow}}} - \underbrace{\int_{t_i}^{t_f} \dot{M}_L h_L dt}_{\substack{\text{Energy leaving} \\ \text{through liquid} \\ \text{outflow}}} + \underbrace{\int_{t_i}^{t_f} \dot{Q} dt}_{\substack{\text{Energy from} \\ \text{environment} \\ \text{(Heat leak} \\ \text{from conduc-} \\ \text{tion con-} \\ \text{vection, and} \\ \text{radiation)}}} \quad (D12)$$

The terms of equation (D12) were evaluated in the manner described in the next section.

Energy Input by Pressurant Gas in Flow

The first term in equation (D12) may be evaluated as

$$\int_{t_i}^{t_f} \dot{M}_G h_G dt \approx \sum_{n=0}^{n=(t_f-t_i)/\Delta t} \dot{M}_{G,n} h_{G,n} \Delta t \quad (D13)$$

The pressurant flow rate \dot{M}_G was determined from equation (D4). The specific enthalpy of the inlet gas was evaluated at the inlet temperature and pressure at each time increment (Δt).

Energy Leaving by Liquid Outflow

$$\int_{t_i}^{t_f} \dot{M}_L h_L dt \approx \sum_{n=0}^{n=(t_f-t_i)/\Delta t} \dot{M}_{L,n} h_{L,n} \Delta t \quad (D14)$$

The liquid flow rate \dot{M}_L was determined from the turbine flowmeter. The specific enthalpy of the liquid was evaluated at the outlet temperature.

Energy Input from Environment

The rate of energy input into the tank from the environment was assumed to be the same for all cases and was determined from a boiloff test. This test indicated that a nominal value of 4.87×10^3 joules/second (4.66 Btu/sec) should be used. This value, which includes heat input by radiation, convection and conduction through pipes and supports, was in all test cases less than 11.0 percent of the energy added to the tank by the pressurant gas.

$$\int_{t_i}^{t_f} \dot{Q} dt \approx 4.87 \times 10^3 (t_f - t_i) \quad (D15)$$

Change in System Energy

The change in system energy can be separated into three categories: (1) change in ullage energy, (2) change in liquid energy, and (3) change in the wall energy:

$$dU_T = dU_U + dU_L + dU_w \quad (D16)$$

Change in ullage energy. - The change in the ullage energy over any given time interval ($t_i \rightarrow t_f$) is obtained by subtracting the internal energy of the ullage at time t_i from the internal energy at time t_f :

$$\int_{U_{t_i}}^{U_{t_f}} dU_U = (U_U)_{t_f} - (U_U)_{t_i} \quad (D17)$$

Making use of the relation $U = H - PV$ gives

$$\int_{U_{t_i}}^{U_{t_f}} dU_U = \sum_{V_f} \rho_U \left(h_U - \frac{P}{\rho_U} \right) \Delta V_U - \sum_{V_i} \rho_U \left(h_U - \frac{P}{\rho_U} \right) \Delta V_U \quad (D18)$$

The ullage gas density was determined using equation (D7). The ullage gas enthalpy was calculated using the relation

$$h = \frac{M_{H_2}}{M_T} h_{H_2} + \frac{M_{He}}{M_T} h_{He} \quad (D19)$$

Therefore, by knowing the pressure, temperature, and ullage gas concentration profiles at times t_f and t_i the change in ullage energy was evaluated.

Change in liquid energy. - The change in energy of the liquid in the tank can be determined in a manner similar to the change in ullage energy:

$$\int_{U_{t_i}}^{U_{t_f}} dU_L = (U_L)_{t_f} - (U_L)_{t_i} \quad (D20)$$

$$\int_{U_{t_i}}^{U_{t_f}} dU_L = \sum_{V_f} \rho_L \left(h_L - \frac{P}{\rho_L} \right) \Delta V_L - \sum_{V_i} \rho_L \left(h_L - \frac{P}{\rho_L} \right) \Delta V_L \quad (D21)$$

where the liquid density and enthalpy are functions of pressure and temperature.

Change in wall energy. - The change in wall energy was determined by applying the first law of thermodynamics to an element of the wall

$$\int_{U_{t_i}}^{U_{t_f}} dU_w = \Delta U_w = \Delta M_w \int_{T_1}^{T_2} C_v dT \quad \text{where } C_v = C_v(T) \quad (D22)$$

The total change of the wall is then

$$\Delta U_{w, T} \cong \sum_{M_w} (\Delta U_w)_n \cong \sum_{M_w} \Delta M_w \int_{T_1}^{T_2} C_v(T) dT \quad (D23)$$

Total Energy Change of System

For convenience equation (D16) is substituted into (D12)

$$\int_{t_i}^{t_f} \frac{d}{dt} (U_U + U_w + U_L) dt = \int_{t_i}^{t_f} \dot{M}_G h_G dt - \int_{t_i}^{t_f} \dot{M}_L h_L dt + \int_{t_i}^{t_f} \dot{Q} dt \quad (D24)$$

Rearranging terms results in

$$\underbrace{\int_{t_i}^{t_f} (\dot{M}_G h_G + \dot{Q}) dt}_{\text{Total energy added } (\Delta U_T)} = \underbrace{\int_{t_i}^{t_f} (\dot{M}_L h_L dt + dU_L)}_{\text{Total change in liquid in tank + liquid expelled energy } (\Delta U_L)} + \underbrace{\int_{t_i}^{t_f} dU_U}_{\text{Total change in ullage energy } (\Delta U_U)} + \underbrace{\int_{t_i}^{t_f} dU_w}_{\text{Total change in wall energy } (\Delta U_w)} \quad (D25)$$

and dividing through by ΔU_T gives

$$1 = \frac{\Delta U_L}{\Delta U_T} + \frac{\Delta U_U}{\Delta U_T} + \frac{\Delta U_w}{\Delta U_T} \quad (\text{D26})$$

The data of this report are presented in the form of these ratios. These ratios show the relative distribution of the total energy input.

REFERENCES

1. Roudebush, William H.: An Analysis of the Problem of Tank Pressurization During Outflow. NASA TN D-2585, 1965.
2. Epstein, M.; Georgius, H. K.; and Anderson, R. E.: A Generalized Propellant Tank-Pressurization Analysis. International Advances in Cryogenic Engineering. Vol. 10. K. D. Timmerhaus, ed., Plenum Press, 1965, pp. 290-302.
3. DeWitt, Richard L.; Stochl, Robert J.; and Johnson, William R.: Experimental Evaluation of Pressurant Gas Injectors During the Pressurized Discharge of Liquid Hydrogen. NASA TN D-3458, 1966.
4. Stochl, Robert J.; Masters, Phillip A.; DeWitt, Richard L.; and Maloy, Joseph E.: Gaseous-Hydrogen Requirements for the Discharge of Liquid Hydrogen from a 1.52-Meter- (5-foot-) Diameter Spherical Tank. NASA TN D-5336, 1969.
5. Stochl, Robert J.; Masters, Phillip A.; DeWitt, Richard L.; and Maloy, Joseph E.: Gaseous-Hydrogen Pressurant Requirements for the Discharge of Liquid Hydrogen from a 3.96-Meter- (13-foot-) Diameter Spherical Tank. NASA TN D-5387, 1969.
6. Stochl, Robert J.; Maloy, Joseph E.; Masters, Phillip A.; and Dewitt, Richard L.: Gaseous-Helium Requirements for the Discharge of Liquid Hydrogen from a 1.52-Meter- (5-Ft-) Diameter Spherical Tank. NASA TN D-5621, 1970.
7. Stochl, Robert J.; and DeWitt, Richard L.: Temperature and Liquid-Level Sensor for Liquid-Hydrogen Pressurization and Expulsion Studies. NASA TN D-4339, 1968.
8. Roellig, Leonard O.; and Giese, Clayton: Solubility of Helium in Liquid Hydrogen. J. Chem. Phys., vol. 37, no. 1, July 1, 1962, pp. 114-116.
9. Gluck, D. F.; and Kline, J. F.: Gas Requirements in Pressurized Transfer of Liquid Hydrogen. Advances in Cryogenic Engineering. Vol. 7. K. D. Timmerhaus, ed., Plenum Press, 1962, pp. 219-233.
10. Olsen, William A., Jr.: Analytical and Experimental Study of Three Phase Heat Transfer with Simultaneous Condensing and Freezing on Cold Horizontal and Vertical Plates. Ph.D. Thesis, Univ. Connecticut, 1967.
11. Kays, W. M.: Convective Heat and Mass Transfer. McGraw-Hill Book Co., Inc., 1966.
12. Dickson, Philip F.: Large Gradient Mass Transfer. Ph.D. Thesis, Univ. Minnesota, 1962.

13. McAdams, William H.: Heat Transmission. Third ed., McGraw-Hill Book Co., Inc., 1954.
14. Olsen, William A.: Experimental and Analytical Investigation of Interfacial Heat and Mass Transfer in a Pressurized Tank Containing Liquid Hydrogen. NASA TN D-3219, 1966.
15. Dodge, Barnett F.: Chemical Engineering Thermodynamics. McGraw-Hill Book Co., Inc., 1944, pp. 183-186.

NATIONAL AERONAUTICS AND SPACE ADMINISTRATION
WASHINGTON, D. C. 20546
OFFICIAL BUSINESS

FIRST CLASS MAIL



POSTAGE AND FEES PAID
NATIONAL AERONAUTICS AND
SPACE ADMINISTRATION

07U 001 53 51 3DS 70348 00903
AIR FORCE WEAPONS LABORATORY /WLOL/
KIRTLAND AFB, NEW MEXICO 87117

ATT E. LOU BOWMAN, CHIEF, TECH. LIBRARY

POSTMASTER: If Undeliverable (Section 1:
Postal Manual) Do Not Ret

"The aeronautical and space activities of the United States shall be conducted so as to contribute . . . to the expansion of human knowledge of phenomena in the atmosphere and space. The Administration shall provide for the widest practicable and appropriate dissemination of information concerning its activities and the results thereof."

— NATIONAL AERONAUTICS AND SPACE ACT OF 1958

NASA SCIENTIFIC AND TECHNICAL PUBLICATIONS

TECHNICAL REPORTS: Scientific and technical information considered important, complete, and a lasting contribution to existing knowledge.

TECHNICAL NOTES: Information less broad in scope but nevertheless of importance as a contribution to existing knowledge.

TECHNICAL MEMORANDUMS: Information receiving limited distribution because of preliminary data, security classification, or other reasons.

CONTRACTOR REPORTS: Scientific and technical information generated under a NASA contract or grant and considered an important contribution to existing knowledge.

TECHNICAL TRANSLATIONS: Information published in a foreign language considered to merit NASA distribution in English.

SPECIAL PUBLICATIONS: Information derived from or of value to NASA activities. Publications include conference proceedings, monographs, data compilations, handbooks, sourcebooks, and special bibliographies.

TECHNOLOGY UTILIZATION PUBLICATIONS: Information on technology used by NASA that may be of particular interest in commercial and other non-aerospace applications. Publications include Tech Briefs, Technology Utilization Reports and Notes, and Technology Surveys.

Details on the availability of these publications may be obtained from:

SCIENTIFIC AND TECHNICAL INFORMATION DIVISION
NATIONAL AERONAUTICS AND SPACE ADMINISTRATION
Washington, D.C. 20546